

1

DETERMINATION OF EARTHQUAKE INTENSITIES FROM CHIMNEY DAMAGE REPORTS

by

ALAN DARRELL HO

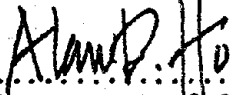
B.Arch., University of Illinois Chicago Circle
(1977)

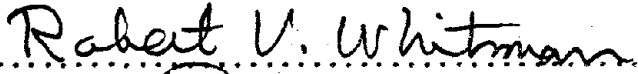
Submitted in partial fulfillment
of the requirements for the degree of
Master of Science in Civil Engineering

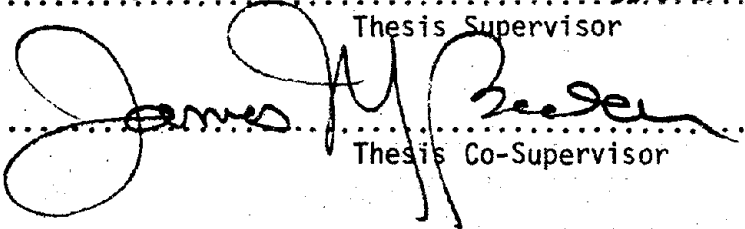
at the

Massachusetts Institute of Technology
June, 1979

© Massachusetts Institute of Technology 1979

Signature of Author..... 
Department of Civil Engineering, June, 1979

Certified by..... 
Thesis Supervisor

..... 
Thesis Co-Supervisor

Accepted by.....
Chairman, Departmental Committee on Graduate Students
of the Department of Civil Engineering

Any opinions, findings, conclusions
or recommendations expressed in this
publication are those of the author(s)
and do not necessarily reflect the views
of the National Science Foundation.

REPORT DOCUMENTATION PAGE	1. REPORT NO. NSF/RA-790705	2.	3. Recipient's Accession No. PB82 103441
4. Title and Subtitle Determination of Earthquake Intensities from Chimney Damage Reports		5. Report Date June 1979	
7. Author(s) R.V. Whitman, PI, J.M. Becker, A.D. Ho		6.	
9. Performing Organization Name and Address Massachusetts Institute of Technology Department of Civil Engineering Cambridge, MA 02139		8. Performing Organization Rept. No.	
12. Sponsoring Organization Name and Address Engineering and Applied Science (EAS) National Science Foundation 1800 G Street, N.W. Washington, DC 20550		10. Project/Task/Work Unit No.	
15. Supplementary Notes Submitted by: Communications Program (OPRM) National Science Foundation Washington, DC 20550		11. Contract(C) or Grant(G) No. (C) (G) ENV7715331	
16. Abstract (Limit: 200 words) An approach to determine earthquake intensities from chimney damage reports is presented. In particular, the intensity of Boston's Cape Ann Earthquake of November 18, 1755, is estimated. A detailed analysis of a two-story, heavy-timber frame house with a masonry chimney extant in 1755 was performed to determine (1) the dynamic response characteristics; (2) force levels in the structure when subjected to earthquake motions; (3) forces required to initiate damage; and (4) the approximate (lower bound) intensity of the 1755 earthquake. A standard analytical model, with basic mass and stiffness properties, was developed and a parametric study was performed to analyze the effects of the several chimney, house, and ground parameters involved in the study. Results indicated that the chimney-house system was quite stiff with a fundamental frequency of about 12 Hz. It was also observed that the higher modes contributed to the total response of the system. The effect of a gap in the chimney-house connection appeared to be an important consideration in determining chimney damage due to earthquakes. It was concluded that an earthquake intensity in the range of 0.15g to 0.04g would initiate damage to the various chimneys as modeled.		13. Type of Report & Period Covered MS Thesis	
17. Document Analysis a. Descriptors Earthquake resistant structures Earthquakes Chimneys b. Identifiers/Open-Ended Terms Cape Ann Earthquake of 1755 Boston (Massachusetts) c. COSATI Field/Group		Houses Damage assessment Dynamic response	
18. Availability Statement NTIS	19. Security Class (This Report)	21. No. of Pages	
	20. Security Class (This Page)	22. Price	

ABSTRACTDETERMINATION OF EARTHQUAKE INTENSITIES FROM CHIMNEY DAMAGE REPORTS

by

Alan Darrell Ho

Submitted to the Department of Civil Engineering on June 25, 1979, in partial fulfillment of the requirements for the degree of Master of Science.

An approach to determining earthquake intensities from chimney damage reports is presented. In particular, the intensity at Boston of the Cape Ann Earthquake of November 18, 1755 is estimated. A detailed analysis of a two story heavy timber brame home with a masonry chimney extant in 1755 was performed to determine i) the dynamic response characteristic ii) force levels in the structure when subjected to 3 earthquake motions iii) forces required to initiate damage and iv) the approximate (lower bound) intensity of the 1755 Earthquake. A standard analytical model, with basic mass and stiffness properties, was enveloped and a parametric study was performed to understand the effects of the several chimney, house and ground parameters involved in the study.

The results indicate that the chimney-house system is quite stiff with a fundamental frequency of about 12 Hz. It was also observed that the higher modes contribute to the total response of the system. The effect of a gap in the chimney-house connection appears to be a very important consideration in determining chimney damage due to earthquakes.

It is concluded that an earthquake intensity in the range of 0.15g to 0.04g would initiate damage to the various chimneys as modeled.

Thesis Supervisor

Robert V. Whitman
Professor of Civil Engineering

Thesis Co-Supervisor

James M. Becker
Associate Professor of Civil Engineering

ACKNOWLEDGEMENT

The author wishes to express his deepest gratitude to Professors Robert V. Whitman and James M. Becker for their invaluable engineering judgement, guidance and patience in preparing this work. Acknowledgement is also made to friends at M.I.T. and particularly his colleagues in Room 1-245 who gave him encouragement. Finally, Mrs. Jessica Malinofsky, Ms. Stephanie Demeris and Ms. Donna Masone deserve high praise for their wonderful typing.

This research project is supported under the National Science Foundation Earthquake Hazards Mitigation Program. "Analysis of the Cape Ann Earthquake from Building Damage". NSF Program Officer: Dr. John Scalzi Grant No. ENV77-15331.

TABLE OF CONTENTS

	<u>Page</u>
Title Page	1
Abstract	2
Acknowledgements	3
Lists of Figures and Tables	6
CHAPTER 1 - Introduction	8
1.1 General	8
1.2 Scope of Thesis	9
1.3 Organization of Thesis	11
CHAPTER 2 - Chimney Analysis	16
2.1 Introduction	16
2.2 Description of Typical Heavy-Timber Frame House Extant in 1755	16
2.3 Preliminary Analysis and Behavior	18
2.4 Standard Analytical Model	20
2.5 Description of DRAIN 2-D and EIGZF	23
2.6 Parametric Study	25
CHAPTER 3 - Analysis Results	49
3.1 Introduction	49
3.2 Free Vibration Analysis	49
3.2a Chimney Parameters	49
3.2b House Parameters	50
3.2c Ground Parameters	50
3.3 Dynamic Analysis Results	51
3.3a Chimney Parameters	52
3.3b House Parameters (except impact)	53
3.3c Impact	55
CHAPTER 4 - Earthquake Intensities	82
4.1 Introduction	82
4.2 Failure Criteria	82

TABLE OF CONTENTS (Continued)

	<u>Page</u>
4.3 Earthquake Intensities	84
4.3a Chimney Parameters	84
4.3b House Parameters	85
4.3c Ground Parameters	86
4.3d Impact	86
CHAPTER 5 - Conclusions and Recommendations	90
5.1 Conclusions	90
5.2 Recommendations	92
APPENDIX A - Method for Predicting the Lateral Stiffness and Strength of Multi-story Infilled Frames	94
APPENDIX B - Spring Constants for Rigid Rectangular Base Resting on Elastic Half-Space	97
APPENDIX C - Gap Model Time Step Accuracy and Scaling of Results	100
REFERENCES	105

LIST OF FIGURES

<u>FIGURE NO.</u>	<u>TITLE</u>	<u>PAGE</u>
1.1	Forces Acting on Tombstone	12
1.2	Isoseismal Map Earthquake of November 18, 1955	13
2.1a	Whipple-Matthews House First Floor Plan	28
2.1b	Chimney Plans	29
2.1c	Chimney Elevations	30
2.1d	Chimney Sections	31
2.2	Corbel Detail	32
2.3	Floor-Chimney Detail	33
2.4	Mortise and Tenon Joint	34
2.5	Exterior Wall Details	35
2.6	Elevation of Chimney	36
2.7	Standard Analytical Model Finite Element Assemblage	39
2.8	Equivalent Strut Concept	41
2.9	Whipple-Matthews House Time Truss Longitudinal Direction	42
2.10a	Truss Element Yielding Tension & Compression	43
2.10b	Beam Element Moment Rotation Relationship	43
2.10c	Semi-Rigid Connection Element (Rocking Spring Element) Moment Rotation Relationship.	44
2.10d	Impact Element (Modified Shear Connection Element) Force Displacement Relationship	44
2.11a	Response Spectrum, El Centro	45
2.11b	Response Spectrum, Ferndale	46
2.11c	Response Spectrum, Palmdale	47
3.1	Standard Model Mode Shapes	58
3.2	Frequency vs. Modulus	63
3.3	Element 3 Shear Force vs. Elastic Modulus	64
3.4	Element 3 Shear Force vs. Gap Size	65
4.1	Shear Failure	88
4.2	Normal Stress Failure	88
A.1	Effective Width as a Function of λh	95
B.1	Spring Constant Coefficients for Rectangular foundations	98

LIST OF TABLES

<u>TABLE NO.</u>	<u>TITLE</u>	<u>PAGE</u>
1.1	The Modified Mercalli Intensity Scale	14
2.1	Preliminary Model Mass and Geometric Properties	37
2.2a	Preliminary Model Fundamental Frequencies	38
2.2b	Preliminary Model Participation Factors	38
2.3	Standard Model Mass and Geometric Properties	40
2.4	Parametric Study	48
3.1	Natural Frequencies	57
3.2a	Shear Force Results, El Centro	66
3.2b	Moment Results, El Centro	67
3.2c	Shear Force Results, Ferndale	68
3.2d	Moment Results, Ferndale	69
3.2e	Shear Force Results, Palmdale	70
3.2f	Moment Results, Palmdale	71
3.2g	Gap Model Shear Force Results, El Centro	72
3.2h	Gap Model Moment Results, El Centro	73
3.2i	Gap Model Shear Force Results, Ferndale	74
3.2j	Gap Model Moment Results, Ferndale	75
3.2k	Gap Model Shear Force Results, Palmdale	76
3.2l	Gap Model Moment Results, Palmdale	77
3.3a	Average Shear Force Results	78
3.3b	Average Moment Results	79
3.3c	Gap Model Average Shear Force Results	80
3.3d	Gap Model Average Moment Results	81
4.1	Failure Force (Shear)	89
4.2	Failure Moment	89
C.1	Shear Forces Comparing Time Steps (0.01 and 0.05 sec.)	101
C.2	Shear Forces Comparing Time Steps (0.0008 and 0.001 sec.)	102
C.3	Shear Forces Comparing Time Steps (0.0008 and 0.0005 sec.)	103
C.4	Shear Forces Indicating Scaling of Gap Model	104

CHAPTER 1 - INTRODUCTION

1.1 General

In the past, and still today where seismographs are not available, the intensity of an earthquake has been expressed in terms of observations of natural phenomena and the extent of damage to structures. The widely used Modified Mercalli (MM) scale, Table 1.1, which is a 12-point scale ranging from I, not felt by anyone, to XII, total destruction, is an example of such an intensity scale. But such subjective intensity scales are deficient in providing criteria such as peak ground acceleration, frequency content, duration, velocity and displacement, for the design of earthquake-resistant structures.

Observations of damaged structures have been utilized to obtain a quantitative approximation to the intensity, expressed in terms of maximum ground acceleration. As an example, the Japanese have observed the final position of displaced tombstones in an attempt to obtain the maximum ground acceleration of an earthquake [1.1]. The method is briefly described below.

If it is assumed that the inertial force acting on the tombstone at the time of maximum ground acceleration is applied statically, the relation between seismic and gravitational forces at the instant when the tombstone is on the verge of overturning will be as indicated in Fig. 1.1. By summing moments about point D, the ground acceleration required to initiate overturning may be obtained in terms of the tombstone dimensions, Eq. (1.1).

$$Mx \frac{h}{2} = W \frac{b}{2} \quad (1.1)$$

$$\frac{x}{g} = \frac{b}{h}$$

Thus by going to a cemetery after an earthquake and examining the ratios of base width and height of tombstones a general idea of the intensity of an earthquake is obtained. Although this method is convenient, the soil conditions in a cemetery are usually poorer than that in surrounding areas. Moreover, the events leading to a displaced or overturned tombstone are not always the same. In any case, this treatment of overturning considers seismic forces, which really act dynamically, as being static; so it is only a method of rough approximation.

1.2 Scope of Thesis

The present work is an effort toward determining earthquake intensities from chimney damage reports. The main objective of this thesis is to understand the dynamic response characteristics of a pre-1755 masonry chimney and its interaction with a heavy timber frame house (also pre-1755), in order to estimate the intensity of the November 18, 1755 Earthquake in New England. The "1755 Earthquake," whose epicenter is thought to have been located about 10 miles east of Cape Ann, Massachusetts, is one of the larger earthquakes in New England's seismic history. With an epicentral intensity of MM VIII, it was felt from Halifax, Nova Scotia, to the northeast and from Annapolis, Maryland, to the southwest, and was reported inland to Fort Crown Point, New York, as shown in Figure 1.1.

A significant amount of chimney damage was reported after the earthquake. Damage appeared to be heaviest in the region around Cape Ann and Boston, Massachusetts, although it was observed that in Boston much of the damage was confined to the area of infilling near the wharves. One account reports [1.2] that "... about one hundred chimneys were in a

manner leveled with the roofs of the houses, and about fifteen hundred shattered and thrown down in part. In some places, especially upon the low, loose ground made by encroachments on the harbor, the streets were almost covered with the bricks that had fallen." It also appeared that chimneys were damaged in a few different ways. Damage reports indicate that "... in many instances the portion of the chimney above the roofline toppled over, sometimes causing roofs to cave in." In other instances the portion of the chimney above the roofline was "... partly turned around, as upon a swivel..." or "... shoved on one side horizontally, jutting over, and just nodding to their fall."

In performing a dynamic analysis on a typical residence extant in 1755, it is necessary to make several estimates regarding the condition of the structure. Several factors such as workmanship, weathering, and load history influence the ability of the structure to resist load. Variables such as wall and partition layout, connection details, and soil conditions influence the response of the structure to seismic loads. Strengths and constituents of materials employed at that time significantly affect the degree of damage sustained by the structure.

In order to understand the effect of some of the variables on the chimneys, a parametric study was performed. The study involved developing an analytical model of the house chimney system by estimating some basic mass and stiffness properties and performing a dynamic analysis subjecting the system to three different earthquake motions, all scaled to 1.0g. After obtaining results, one parameter, such as the modulus of elasticity for the masonry or mass distribution of the house, was changed and the analysis performed over again. The results of the parametric study are presented in Chapter 3.

The intensity required to initiate failure of the chimneys was then obtained by first defining a simple failure criterion and determining the forces required to initiate that type of failure. The ratio of the failure forces to the force results of the parametric study is the intensity required to initiate failure. The intensities are tabulated in Chapter 4.

In spite of the several variables involved in this study, it would be interesting to investigate the dynamic response characteristics of a house-chimney system. Moreover, such an investigation seems potentially useful in developing detailed engineering data for contemporary aseismic design.

1.3 Organization of Thesis

Chapter 2 describes the chimney, house and related parameters to be analyzed. Particular attention is paid to developing the basic analytical model, from the architectural and structural details, for the dynamic analysis. The computer programs, DRAIN 2-D and EIGZF, which are used in the analysis, are described. The parametric study is outlined in detail.

Chapter 3 discusses the dynamic response characteristics of the various models of the parametric study. The frequency and mode shapes for the various chimneys are presented. Tabulated force results, for each of the chimneys analyzed, are also presented. Comments are made on the force levels of each model.

Chapter 4 defines the failure criteria used in determining the earthquake intensities. Tabulated earthquake intensities are presented and comments are made on the intensities computed for each model.

Chapter 5 consists of a brief summary of the major conclusions in this study, with some suggestions for future work.

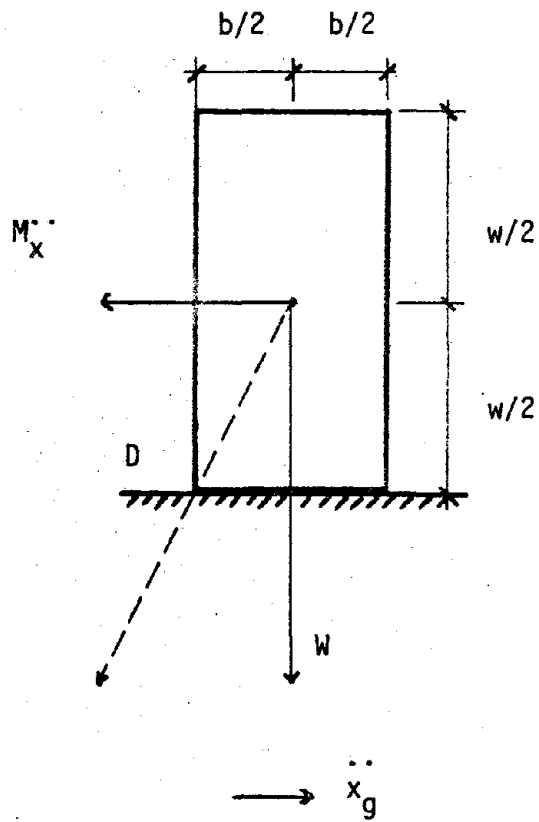


Figure 1.1 Forces acting on tombstone

Page 13 has been removed.

Due to copyright and legibility problems, the following map (Figure 1.2) has been omitted:

Isóseismal Map of Earthquake of November 18, 1755,
prepared by Weston Geophysical Research, Inc.

TABLE 1.1
 THE MODIFIED MERCALLI
 INTENSITY SCALE

Modified Mercalli Intensity Scale of 1931 (Abridged and Rewritten by C.F. Richter).

1. Not felt. Marginal and long-period of large earthquakes.
2. Felt by persons at rest, on upper floors, or favorably placed.
3. Felt indoors. Hanging objects swing. Vibration like passing of light trucks. Duration estimated. May not be recognized as an earthquake.
4. Hanging objects swing. Vibration like passing of heavy trucks; or sensation of a jolt like a heavy ball striking the walls. Standing motor cars rock. Windows, dishes, doors rattle. Glasses clink. Crockery clashes. In the upper range of 4, wooden walls and frames crack.
5. Felt outdoors; direction estimated. Sleepers wakened. Liquids disturbed, some spilled. Small unstable objects displaced or upset. Doors swing, close, open. Shutters, pictures move. Pendulum clocks stop, start, change rate.
6. Felt by all. Many frightened and run outdoors. Persons walk unsteadily. Windows, dishes, glassware broken. Knickknacks, books, and so on, off shelves. Pictures off walls. Furniture moved or overturned. Weak plaster and masonry D cracked. Small bells ring (church, school). Trees, bushes shaken visibly, or heard to rustle.
7. Difficult to stand. Noticed by drivers of motor cars. Hanging objects quiver. Furniture broken. Damage to masonry D including cracks. Weak chimneys broken at roof line. Fall of plaster, loose bricks, stones, tiles, cornices, unbraced parapets, and architectural ornaments. Some cracks in masonry C. Waves on ponds; water turbid with mud. Small slides and caving in along sand or gravel banks. Large bells ring. Concrete irrigation ditches damaged.
8. Steering of motor cars affected. Damage to masonry C; partial collapse. Some damage to masonry B; none to masonry A. Fall of stucco and some masonry walls. Twisting, fall of chimneys, factory stacks, monuments, towers, elevated tanks. Frame houses moved on foundations if not bolted down; loose panel walls thrown out. Decayed piling broken off. Branches broken from trees. Changes in flow or temperature of springs and wells. Cracks in wet ground and on steep slopes.

9. General panic. Masonry D destroyed; masonry C heavily damaged, sometimes with complete collapse; masonry B seriously damaged. General damage to foundations. Frame structures, if not bolted, shifted off foundations. Frames racked. Conspicuous cracks in ground. In alluviated areas sand and mud ejected, earthquake fountains, sand craters.
10. Most masonry and frame structures destroyed with their foundations. Some well-built wooden structures and bridges destroyed. Serious damage to dams, dikes, embankments. Large landslides. Water thrown on banks of canals, rivers, lakes, etc. Sand and mud shifted horizontally on beaches and flat land. Rails bent slightly.
11. Rails bent greatly. Underground pipelines completely out of service.
12. Damage nearly total. Large rock masses displaced. Lines of sight and level distorted. Objects thrown into the air.

CHAPTER 2 - CHIMNEY ANALYSIS

2.1 Introduction

The objective of this chapter is to describe the preparatory work necessary to estimate the intensity of the 1755 Earthquake. A brief description of a typical heavy timber frame house extant in 1755 is provided, along with a summary of a preliminary analysis that was performed to determine the basic behavior of the chimney. This is followed by a description of a standard analytical model that was developed. A standard analytical model was developed so that a comparison of results could be made when the parameters varied. A description of the computer programs used in the study is included, and an outline of the parametric study is presented.

2.2 Description of Typical Heavy-Timber Frame House Extant in 1755.

The chimney to be analyzed was taken from the Whipple-Matthews House (c. 1638) of Hamilton, MA. [2.1]. Chimneys at that time were usually constructed with clay brick laid in a bed of clay or mud mortar. Lime mortar was not used until 1733 [2.2], but when some lime was available it was used for the exterior portions of the chimney, which required a hard mortar to withstand the weather.

The chimney was not built integrally with the house, but there was probably some contact at each floor level due to floor boards butting up against the chimney. Plans of the house (Fig. 2.1) indicate that there existed a gap, as large as one inch, between the main members and the chimney. A detail (Fig. 2.2) of the framing adjacent to the corbelled hearths on the second floor illustrates the degree contact of the framing

members against the chimney. At the roofline, an opening was roughed out through the rafters, with the sheathing and shingles butting up against the chimney just beneath the drip course, as shown in Figure 2.3.

The Whipple-Matthews home is a typical example of a two-story heavy-timber frame house extant in 1755. The frame was constructed of massive hand-hewn oak members mortised and tenoned together and secured with a peg as shown in Figure 2.4. Members required a large cross-section, because much of it was carved away so that the members could be joined together. A typical member size was 8" x 10", but the largest member was approximately 12" x 15". No nails were used in the entire construction except for fastening shingles, sheathing and clapboards.

A common exterior wall section was 3" x 3" oak studs spaced at 20" on center; brick nogging laid in a bed of clay mortar, or mud between the studs, and clapboards nailed to the studs. Another exterior wall section employed in that time consisted of 3" x 3" oak studs at 20" O.C., a layer of sheathing nailed to the studs, and clapboards nailed to the sheathing. Figure 2.5 illustrates these two wall sections. The interior partitions consisted of vertical oak planks nailed into place.

Although a large portion of the Boston area homes were heavy-timber frame homes (approximately 60% [2.1]), the construction techniques for each were not standard. Member sizes were non-uniform, because the timbers were hand-hewn with an axe. Moreover, member sizes depended upon the availability and sizes of trees. The quality of workmanship in making the timber connections, which probably varied, influenced the lateral stiffness of the house. Mortar strengths varied from that of mud to the various lime mortars that eventually became available. Even after lime became

more plentiful, the proportions of the mortar mix were probably not uniform, and the quality of workmanship, which is crucial in masonry construction, was probably not consistent. The type of exterior wall employed also affects the lateral stiffness of the house. The inclusion of brick nogging could add to the lateral stiffness if the mortar had enough strength, acting as an infill panel between beams and columns. The sheathing, if well nailed, could also contribute to the lateral stiffness through shear-type behavior.

Other factors affecting the variability of material strengths are weathering and load history. Weathering would tend to deteriorate materials, especially mortar and masonry of the portion of the chimney above the roofline, while loadings such as past tremors may have caused cracks, weakening the chimney.

Additional factors that would affect the degree of damage sustained by a chimney include site soil conditions and frequency content, duration, amplitude and periodicity of the ground motion.

Due to the number of variables affecting the strength of the house-chimney system, a parametric study was performed to understand the relation of each parameter to the dynamic response characteristics of the system. A detailed description of the parametric study is presented in Section 2.4.

2.3 Preliminary Analysis and Behavior

In studying damage to structures caused by ground motions, it is essential to consider the structural response. Structural response is highly influenced by the proximity of the fundamental frequency of the

system to the predominant frequency of the ground motion. For the chimney-house system, the chimney is basically a very rigid structure, with a high fundamental frequency, while the timber frame can be characterized as a flexible, relatively low fundamental frequency structure.

A preliminary analysis [2.3] of the Whipple-Matthews chimney was performed. For simplification, the chimney was idealized as a cantilever beam (including shear deformation) with seven lumped masses as shown in Figure 2.6. The analysis was performed for six different cases of the chimney: i) chimney only, ii) chimney plus additional lumped mass due to a sheathing and clapboard exterior-wall-type house, as shown in Figure 2.5, and iii) chimney plus lumped mass due to a brick nogging and clapboard exterior-wall-type house, as shown in Figure 2.5. Each of the above-mentioned chimneys was analyzed in both strong and weak bonding axis directions. Table 2.1 indicates the mass and geometric properties of the six chimney types. The two wall types were included in the model to understand their contribution to the dynamic response. By lumping the additional masses due to the walls at each floor level, it is implied that i) the house contributes mass but no stiffness to the system, and ii) the walls, including framing, are in direct contact with the chimney. The first assumption is made to simplify the model, although the house probably does contribute some lateral stiffness to the system.

The second assumption may not necessarily be accurate at each level due to the possibility of a gap between the chimney and the main framing members. At the roofline, where flashing or some other type of weather-proofing exists, it is reasonable to assume that the chimney and framing are, to some degree, in contact. In any case, the assumption is adequate for and simplifies the preliminary analysis.

The dynamic analysis was performed using STRUDL. STRUDL performs a normal mode analysis, where the physical coordinates of the system are transformed into generalized coordinates, thereby uncoupling the equations of motion. The result is a system of single-degree-of-freedom equations, equal in number to the degrees of freedom in the total system, which are integrated individually by the unconditionally stable constant acceleration method. The total response is then obtained by superimposing the response of each mode. The coordinate transformation also facilitates the computation of frequencies and mode shapes.

The frequencies given in Table 2.2a indicate that the fundamental frequency is quite high, 22 Hz for the chimney only in the strong direction (COSD), and 18.2 Hz for the chimney only in the weak direction (COWD). Once the mode shapes were obtained, modal participation factors were calculated to determine the contributions of the various modes. The participation factors given in Table 2.2b indicate that, in general, the higher modes are important in contributing to the total response. This rather unusual behavior is a result of having most of the mass concentrated in the lower, rigid portion of the chimney.

2.4 Standard Analytical Model

In the preliminary analysis the Whipple-Matthews House was roughly idealized as a cantilever beam with seven lumped masses. The study investigated the effects of the variation of house mass and orientation to ground motion. In the present study, various chimney, house, and ground parameters are investigated. In response to the many parameters to be investigated, a standard model was developed so that a comparison could

be made when the parameters were varied, as will be described in Section 2.4.

The standard model (Fig. 2.7) has idealized the Whipple-Matthews chimney as a cantilever beam (including shear deformations) with nine lumped masses. The finer discretization in the slender portion of the chimney is employed to model more accurately the distributed mass system at the critical roofline location. The cross-sectional moment of inertia, the cross-sectional area and the shear areas are computed based upon average values for each beam element and are shown in Table 2.3. As a result, each element has constant cross-sectional properties. Although this is only an approximation to the actual variable moment of inertia chimney, it is felt that the effect on the results is negligible. The actual modulus for the clay mortar, mud or lime mortar used in 1755 is not known, so a value of 216,000 ksf was used for the standard model because it is the modulus of masonry commonly used today. The modulus will be varied as described later in the parametric study.

The house was modeled as a timber truss. The total mass of the house was included in the model and lumped according to tributary area at each joint. The standard house mass used is from the sheathing and clapboard-wall-type house described in Section 2.1. The mortise and tenon joints are assumed to be pinned joints. Although there probably exists some degree of friction in the joint, the contribution to the lateral stiffness is relatively small and can therefore be neglected.

In the transverse direction, Figure 2.1, the lateral resistance of the house is composed of four trusses. The analytical model accounts for the lateral stiffness of the four trusses by multiplying the actual cross-

sectional areas of the beams, rafters and columns by four. The total lateral stiffness is necessary to remain consistent with the inclusion of the total house mass. The longitudinal direction, which may be of some significance, is not treated in this study.

A study in the longitudinal direction would involve estimating the lateral stiffness of the structure shown in Figure 2.9. It would also involve a careful treatment of the different chimney-to-house connections, at the roofline and at each floor level (Figure 2.3.). For these reasons, the investigation of the longitudinal direction would be both interesting and necessary in future research work.

In Figure 2.7 the diagonal members represent the contribution of the wall material between the main beams and columns, to the lateral stiffness. The contribution of the wall material to the lateral stiffness of the house was estimated by using the "Equivalent Strut" concept for infill frames. Basically the diagonal stiffness and strength of an infill panel depends upon its dimensions, physical properties and length of contact with the surrounding frame, as shown in Figure 2.8. The method shows [2.4] that this length of contact was governed by the relative stiffness of the infill and frame. The length of contact is treated in a manner similar to a beam on an elastic foundation, where the infill panel corresponds to the elastic foundation and the frame corresponds to the interacting beam. Once the length of contact was obtained, an effective width of the panel was calculated. The effective width of the panel was then replaced by an equivalent strut [see Appendix A]. It should be noted that the equivalent strut has been computed assuming no windows or door openings, so the strut is only an estimate of the diagonal stiffness of the infill material.

The horizontal members of the truss are assumed to be infinitely rigid, in order to neglect axial shortening of the floor members. Moreover, this assumption constrains the mass of the house to accelerate with the chimney mass to which it is connected, allowing cross-checking with the force results of the preliminary analysis for the chimney-plus-house-mass cases.

A rotational spring at the base of the chimney has been included to model foundation rocking. Scholl and Farhoomand [2.5] have determined from pull tests of wood frame structures that as the structure stiffness of a system increases, foundation participation also increases. The standard spring stiffness was calculated (see Appendix B) by assuming that the foundation was a rigid solid rectangular base resting on an elastic half-space [2.6]. The shear modulus for the soil was determined by assuming a shear wave velocity for a stiff till of 1200 ft./sec. and a mass density of 4.2 lb-sec/ft⁴. The actual base is not a solid rectangle, so it was further assumed that the spring constant is directly proportional to the ratio of $I_{\text{actual}}/I_{\text{solid}}$, the actual second moment of the cross-section to the second moment of the cross-section for the solid rectangular base.

2.5 Description of DRAIN 2-D and EIGZF

The computer program DRAIN 2-D was used to perform the dynamic analysis. DRAIN 2-D is a general-purpose inelastic dynamic analysis program for planar structures developed by Kanaan and Powell [2.7]. The elements available in the program exhibit bilinear force deformation relationships, as shown in Figures 2.10.

DRAIN 2-D directly integrates the equations of motion, assuming a constant acceleration within each time step. The constant acceleration method is unconditionally stable, but the time step must be carefully selected to ensure accurate results. The time step used for the parametric study (except impact cases) was 0.005 seconds, while for the impact study a time step of .0008 seconds was used. The time step for the basic parametric study (except impact cases), which is an elastic analysis, was selected by trial and error until the results converged to the final solution. The usual rule of thumb of using $.1T_p$, where T_p is the period of the highest contributing mode, does not produce results for such a stiff system, due to the storage limitations of DRAIN 2-D. The required time step would have been approximately 0.0007 seconds for the standard model and much smaller for the impact studies. Such a small time step would require a tremendous amount of computer storage when integrating an acceleration of 5.0 seconds duration. DRAIN 2-D does not have sufficient storage capacity requirements to perform an analysis with a time step of 0.0007 seconds for a duration of 5.0 seconds. (see Appendix C)

The time step for the impact study, which is an inelastic analysis, was selected by using the smallest possible time step so that the storage capacity was not exceeded, for a duration of 5.0 seconds. It should be mentioned that the peak response for an impact model subjected to Palmdale analyzed at $\Delta t = 0.008$ seconds for a duration of 5.0 seconds occurred at approximately 2.0 seconds. This observation allowed an analysis to be performed at a time step of $\Delta t = .0005$ for a duration of 3.0 seconds. A comparison of the force results, table C.3 indicates an average difference of 4% for the different time steps. It was therefore concluded that a

time step of $\Delta t = 0.0008$ seconds was sufficiently accurate for the analysis.

Since DRAIN 2-D performs direct integration of the equations of motion, which precludes the coordinate transformation necessary to obtain frequencies and mode shapes, the frequencies and mode shapes were obtained using the computer program EIGZF [2.8]. EIGZF computes eigenvalues and eigenvectors for the generalized eigenproblem, $K\phi = \omega M\phi$, where K and M are the stiffness and mass matrix, respectively, of the finite element assemblage. EIGZF first transforms K to upper Hessenberg form and M to upper triangular form. Then K is further transformed into quasi-upper triangular form or upper Hessenberg form with no two consecutive subdiagonal elements being nonzero, while retaining M in upper and triangular form. Finally, output vectors α and β are computed from K and M and the eigenvalues ω are obtained by taking the square root of α_i/β_i . The eigenvectors are automatically obtained by substituting the eigenvalues into the general equation and solving for ϕ . The eigenvectors are normalized so that the largest component has the absolute value 1.

2.6 Parametric Study

Due to the several undeterminables and variables involved in this study, it is necessary to investigate those parameters which might have significant influence on the dynamic behavior of the system. A discussion of the effect of the variation in parameters compared with the corresponding standard model is presented in Chapter 3. The parameters to be investigated can be separated into three categories: i) chimney parameters, ii) house parameters, and iii) ground parameters.

The chimney parameters investigated are the modulus of elasticity of masonry. Values 108,000 ksf, 54,000 ksf and 144 ksf are studied. Since the exterior portion of the chimney may have deteriorated more than the interior, due to weathering, an additional analysis was performed with an elastic modulus of 54,000 ksf above the roofline and 216,000 ksf below the roofline. A modulus of 216,000 ksf is a common modulus for masonry used today.

The house parameters to be investigated are the mass distribution and the connection between the chimney and house. It should be noted that although the transverse stiffness of the house is not known with great certainty, it is not varied because the resulting frequency of the house alone seemed reasonable. The mass of the two wall details described in Section 2.1, the sheathing and clapboard wall and the brick nogging, sheathing and clapboard wall are used. The house connection is modelled in four basic ways. The first assumes the connection to be infinitely rigid. The mass of the chimney and house will consequently accelerate together. The second assumes no connection. The connecting link is given very small (almost zero) axial stiffness, so that the chimney and house respond independently. The third uses the actual dimensions of the horizontal framing members adjacent to the chimney, and the fourth assumes a gap in the chimney-house connection at the roof and floor levels. The gap between the chimney and house framing would permit some independent movement of both the chimney and house. But, if the gap were small enough and/or their relative displacement large enough, the chimney and house could impact against one another. The gap or impact element was modeled using a spring element with the force-deformation relationship shown in

Figure 2.10d. The initial stiffness is assumed to be small, to model the gap, while the hardening branch represents the stiffness of the timber members in contact with the chimney. Various gap sizes of 0.005', 0.01', 0.015', 0.02', 0.04', and 0.05' are investigated to determine the gap size that would cause the most damage.

The ground parameters investigated are the foundation rocking spring and the ground motions to which the model is subjected. The standard foundation rocking spring stiffness assumed a shear wave velocity of 1220 ft/sec, which is for a stiff till. The rocking spring stiffness is arbitrarily varied to 10% and 1% of the standard rocking spring stiffness, to determine when the house begins to restrain the chimney, i.e., the chimney becomes more flexible than the house. The ground motions used in the study are from the 1940 El Centro Earthquake N-S component, the 1951 Northwest California Earthquake N46W component recorded at Ferndale, CA., and the 1971 San Fernando Earthquake, S30W component recorded at Palmdale, CA.

The ground motions were selected to correspond to the magnitude and distance thought to be typical of the 1755 Earthquake. All accelerograms were scaled to 1.0g so that displacements could be obtained from the computer results. At a peak ground acceleration input of 0.37g, the displacements were so small that the computer output indicated displacements at the top chimney node to be 0.000 ft. The response spectrum for the actual (non-scaled) earthquake motions are shown in Figure 2.11.

A summary of the various analyses to be performed is shown in Table 2.4. The results are presented in Chapter 3 with comments and general observations.

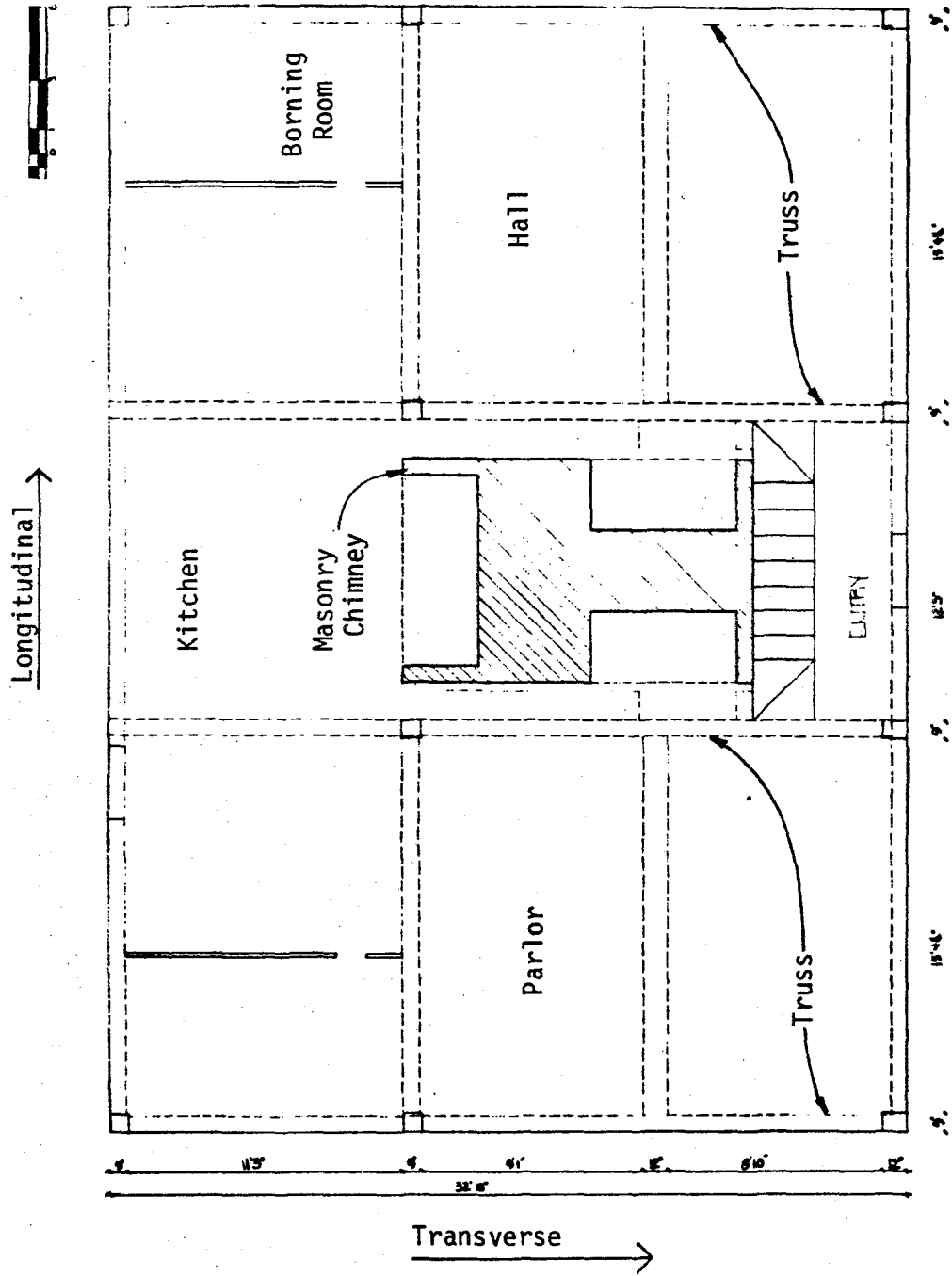


Figure 2.1a Whipple-Matthews House-First Floor Plan

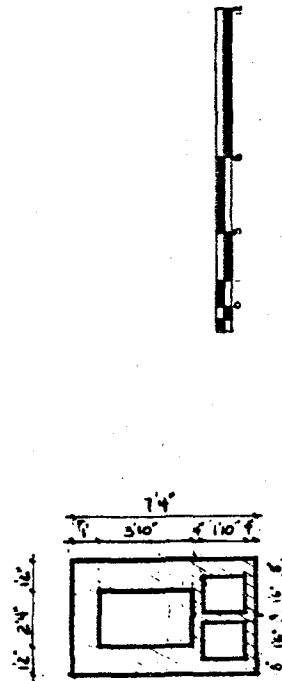
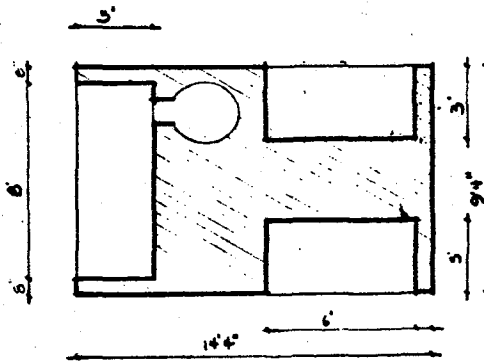
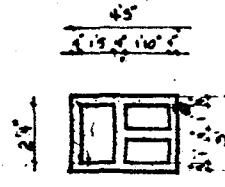
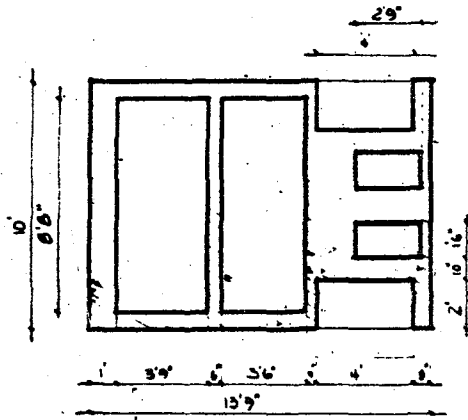


Figure 2.1b Chimney Plans

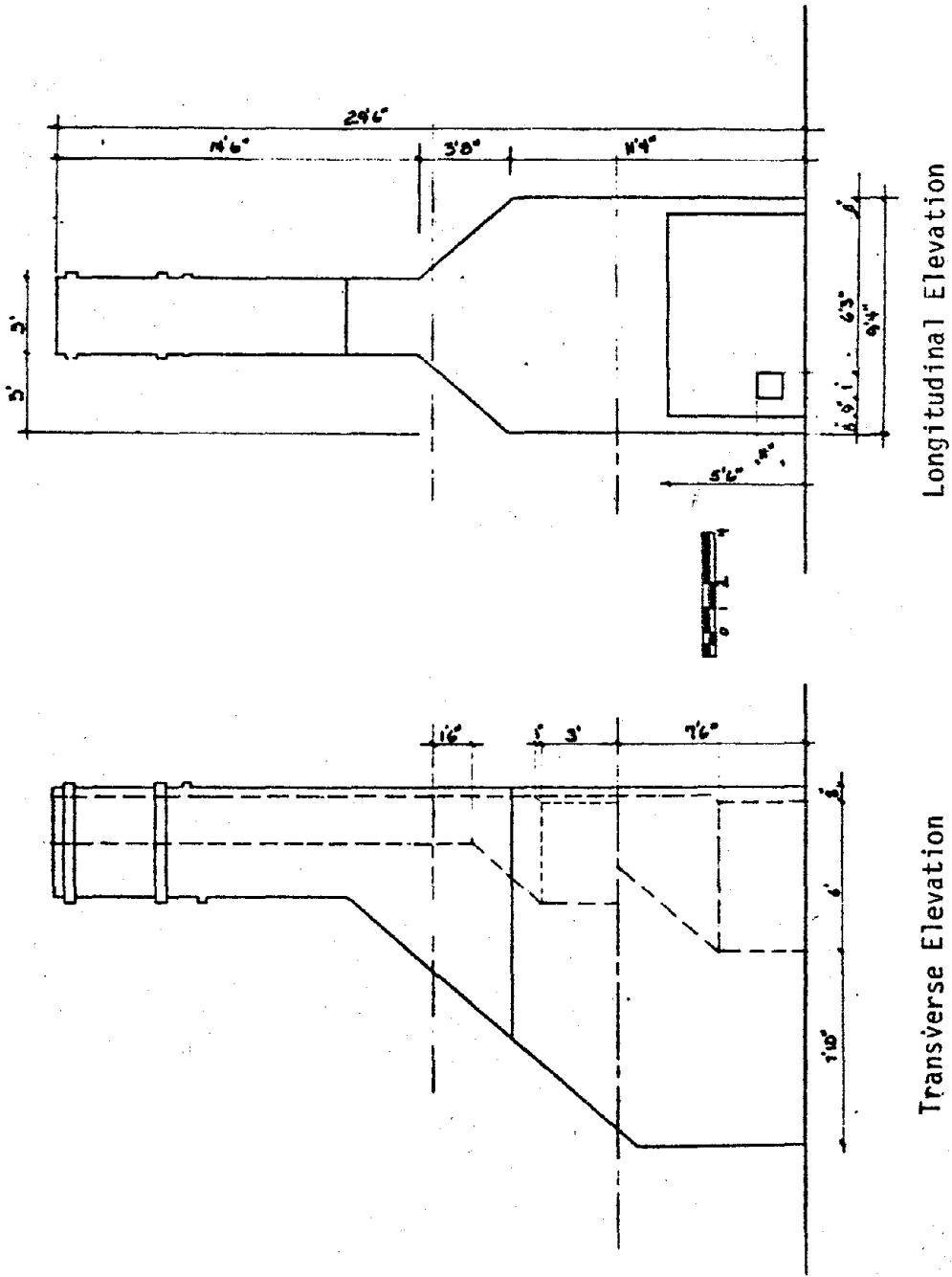


Figure 2.1c Chimney Elevations

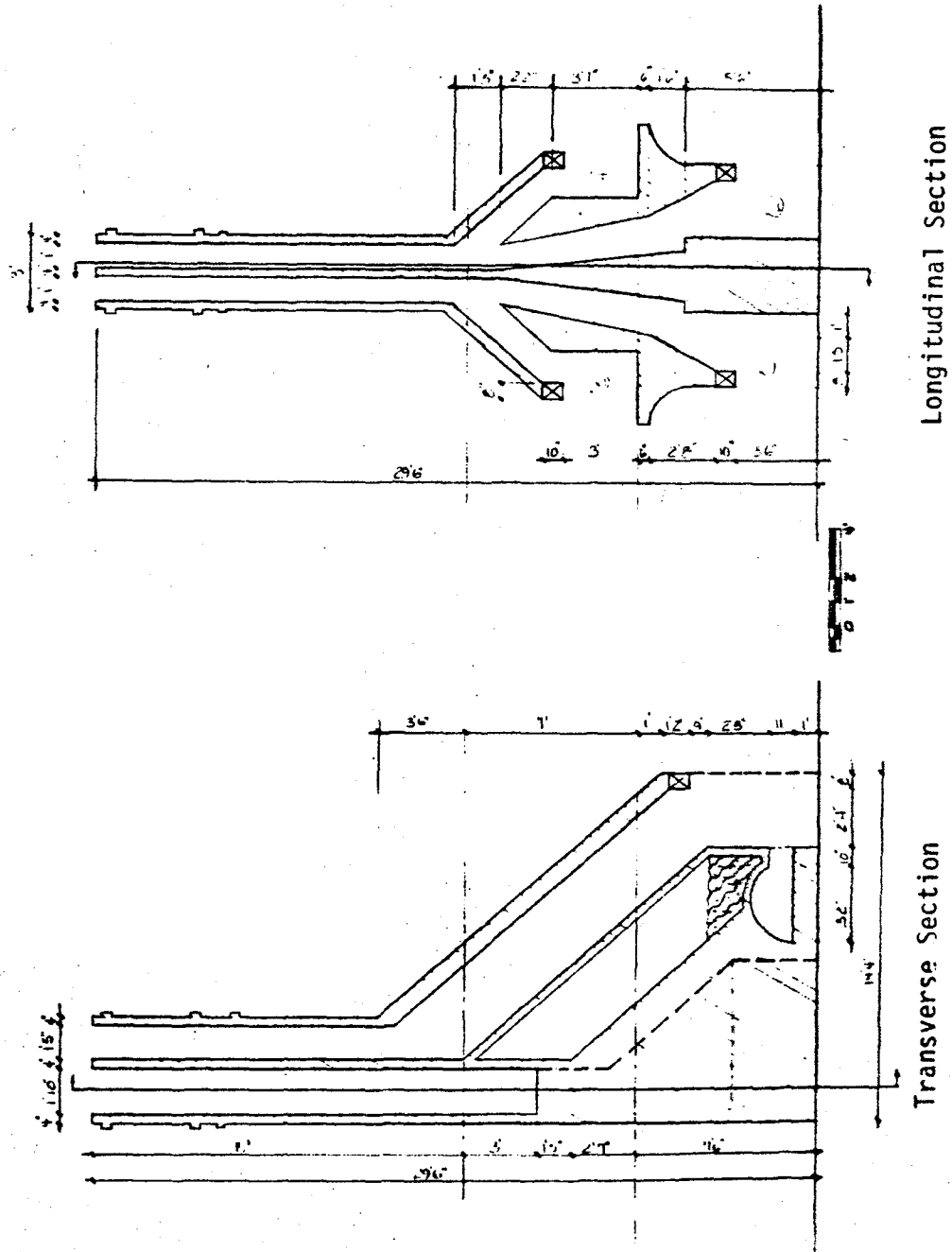


Figure 2.1d Chimney Sections

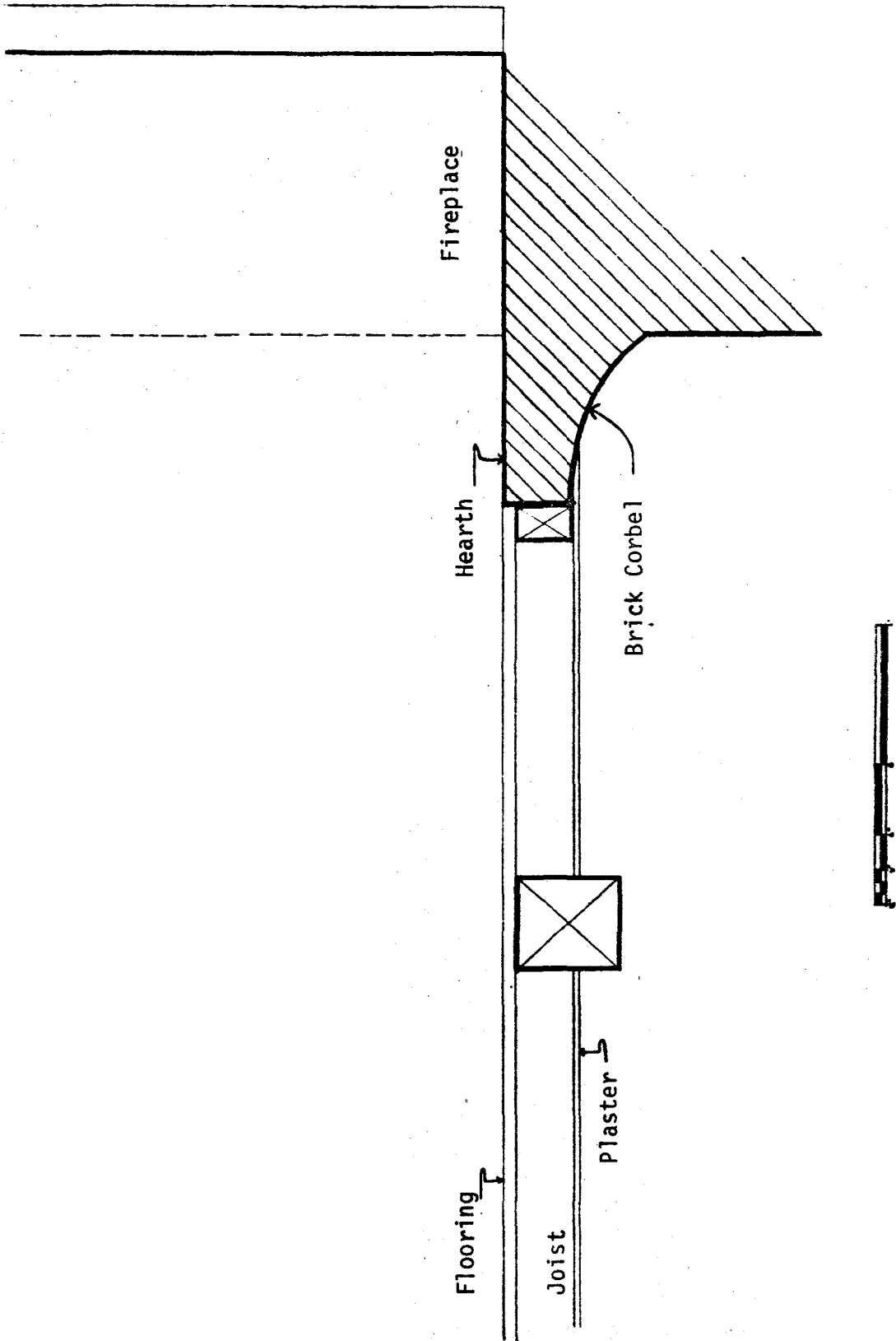


Figure 2.2 Corbel Detail

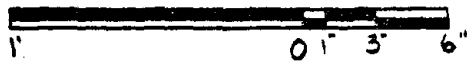
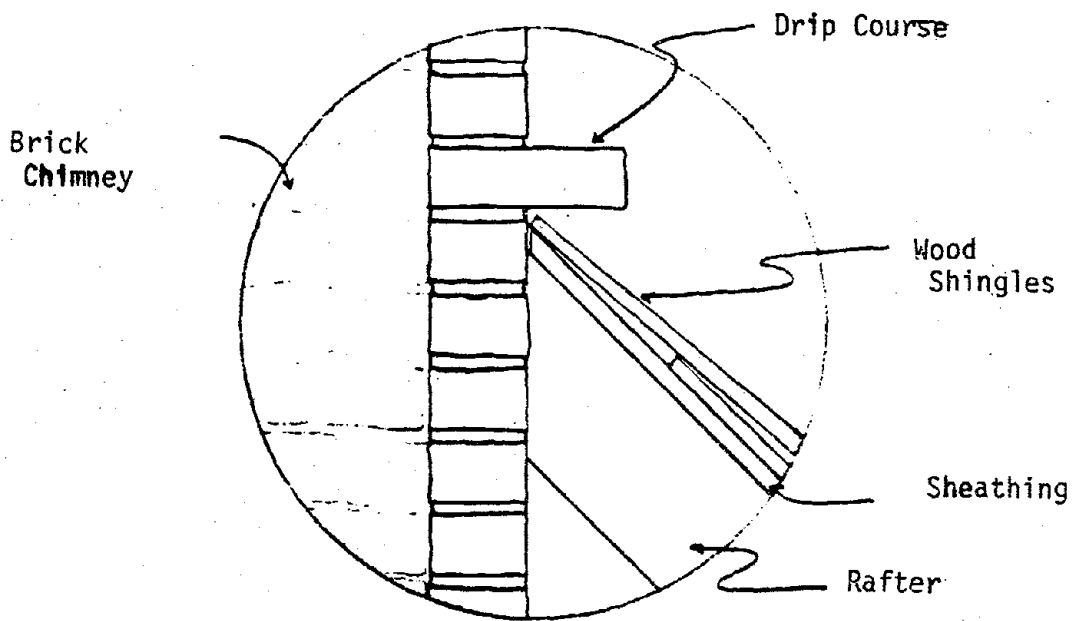


Figure 2.3 - Roof-chimney detail

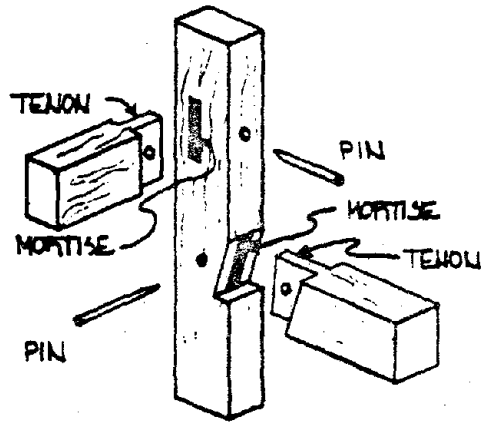


Figure 2.4 Mortise and Tenon Joint

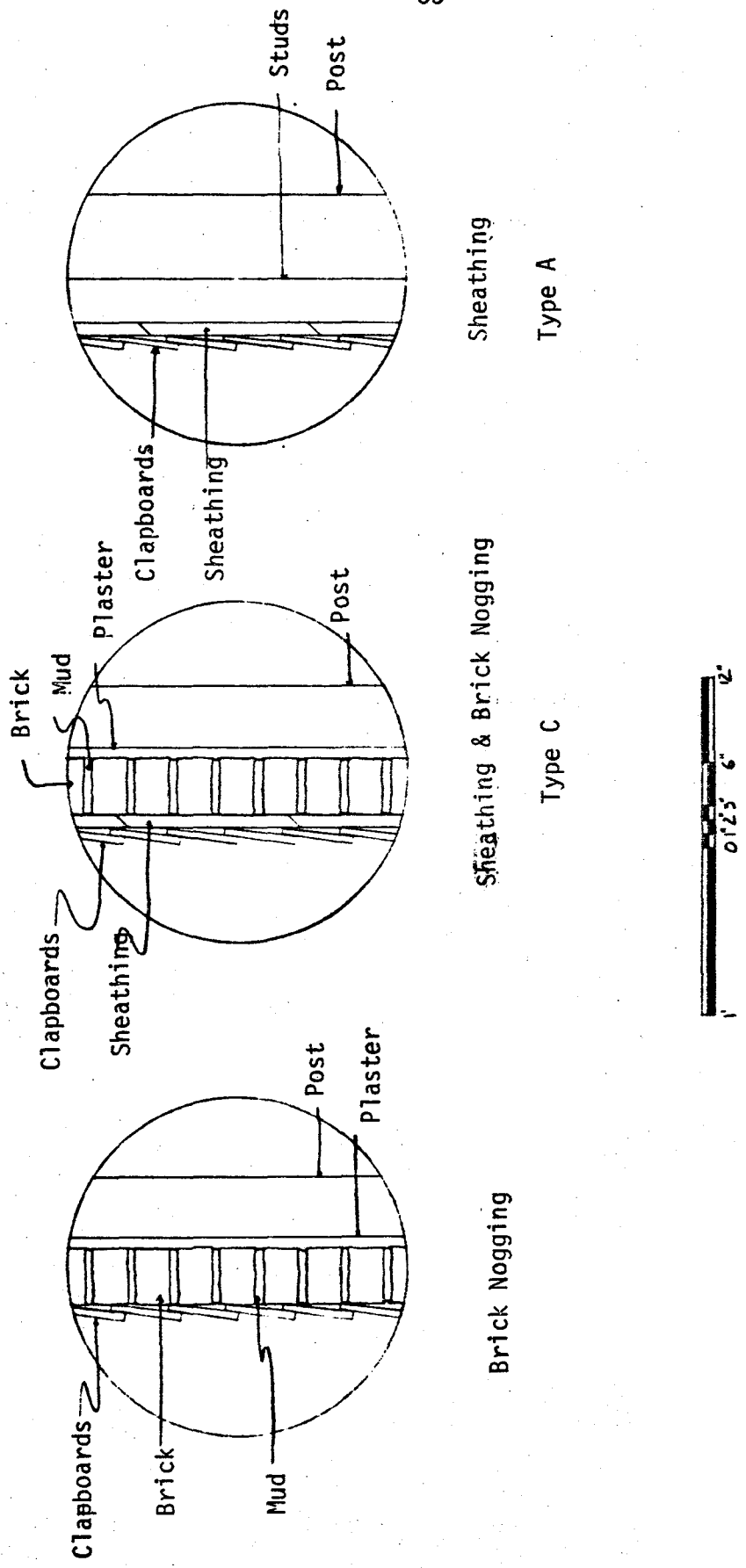


Figure 2:5 - Exterior Wall Details

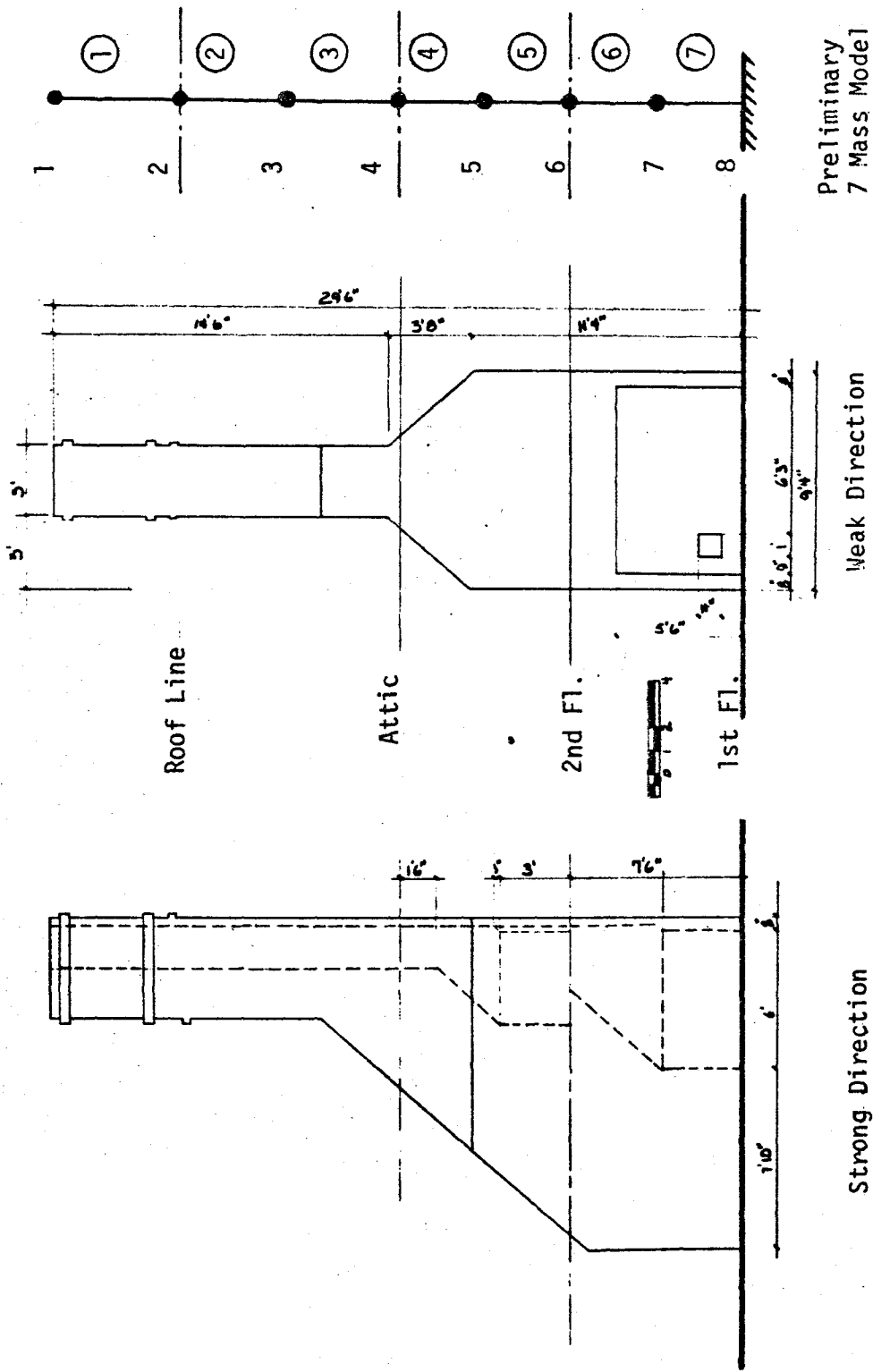


Figure 2.6 Elevation of Chimney

Preliminary Analysis
Whipple-Matthews Chimney
Table 2.1 Mass and Geometric Properties

NODAL MASS* (Slugs)				SECOND MOMENT OF AREA (Ft. ⁴)			ELEMENT
NODE	CO	CA	CC	I _{SD}	I _{WD}	CROSS-SECTIONAL AREA (Ft. ²)	
1	.051	.051	.051	10.8	6.8	5.8	1
2	.097	.572	.724	10.8	6.8	5.8	2
3	.091	.091	.091	10.8	6.8	5.8	3
4	.193	1.299	1.687	257.2	240.0	26.5	4
5	.392	.392	.392	699.5	456.5	41.9	5
6	.585	1.94	2.784	1082.5	535.3	59.7	6
7	.789	.789	.789	1183.3	596.1	68.8	7

* Mass based on 105 lbs/ft³ for masonry

CO = Chimney Only
 CA = Chimney + Wall "A"
 CC = Chimney + Wall "C"
 SD = Strong Direction
 WD = Weak Direction

Table 2.2a Fundamental Frequencies (Hz)[2.3]

COSD	CASD	CCSD	COWD	CAWD	COWD
22	13	12	18	11	10

Table 2.2b Participation Factors

MODE	COSD	CASD	CCSD	COWD	CAWD	CCWD
1	1.8	1.7	1.8	1.8	1.7	1.8
2	-1.6	-1.9	-1.8	-1.4	-1.8	-1.7
3	1.1	1.3	1.6	1.3	1.3	1.6
4	-.85	-1.3	-1.8	-.9	-1.5	-1.6
5	.9	1.7	.95	.9	1.6	1.0
6	-.43	-0.1	-.48	-.27	-0.3	.64
7	.21	.8	1.1	.2	.73	.98

Participation Factor:

$$\Gamma_i = \frac{\sum_j m_j \phi_{ij}}{\sum_j m_j \phi_{ij}^2}$$

; where m_j = mass at node j

ϕ_{ij} = modal deformation at node j in mode i

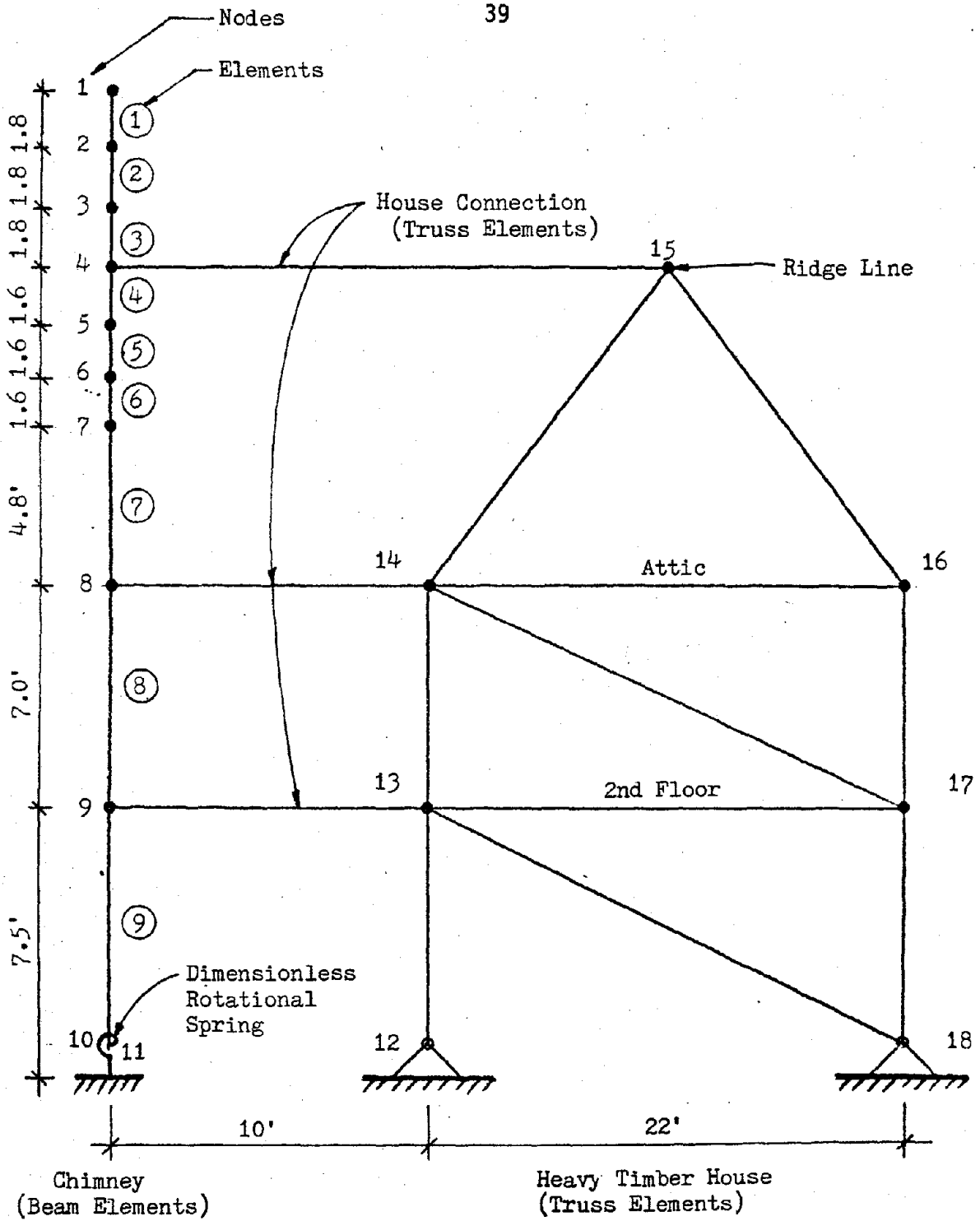
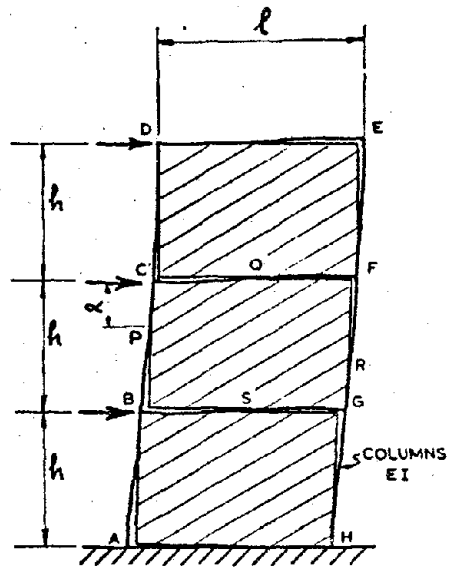


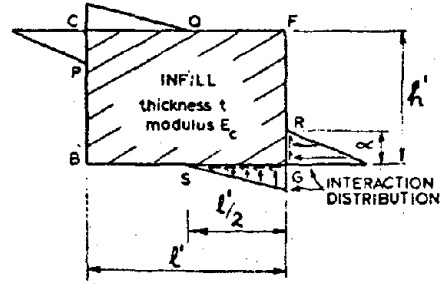
Figure 2.7 Standard Analytical Model
Finite Element Assemblage

Table 2.3 Refined Whipple-Matthews Mass and Geometric Properties

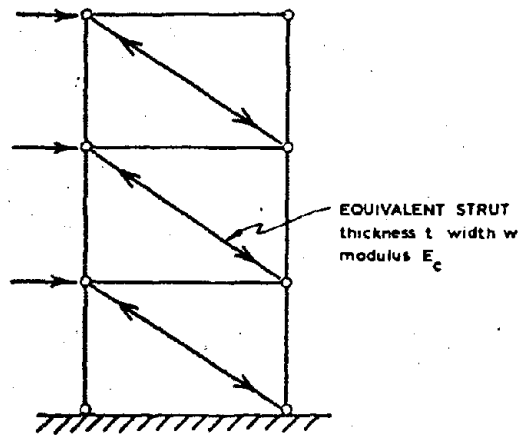
NODE	NODAL MASS (Slugs)			I_{SD} (Ft. ⁴)	Cross Sectional Area (Ft. ²)		ELEMENT
	CO	CA	CC		Shear Area (Ft. ²)		
1	.017	.017	.017	10.8	5.8	13.0	1
2	.034	.034	.034	10.8	5.8	13.0	2
3	.034	.034	.034	10.8	5.8	13.0	3
4	.0323	.5073	.659	10.8	5.8	13.0	4
5	.031	.031	.031	10.8	5.8	13.0	5
6	.031	.031	.031	10.8	5.8	13.0	6
7	.060	.060	.060	42.3	10.9	31.8	7
8	.579	1.691	2.079	468.7	34.1	88.2	8
9	1.17	2.527	3.369	965.2	62.3	152.9	9



(a) INFILLED FRAME



(b) ASSUMED INTERACTION DISTRIBUTION ON TYPICAL INFILL



(c) EQUIVALENT FRAME

Figure 2.8 Equivalent Strut Concept

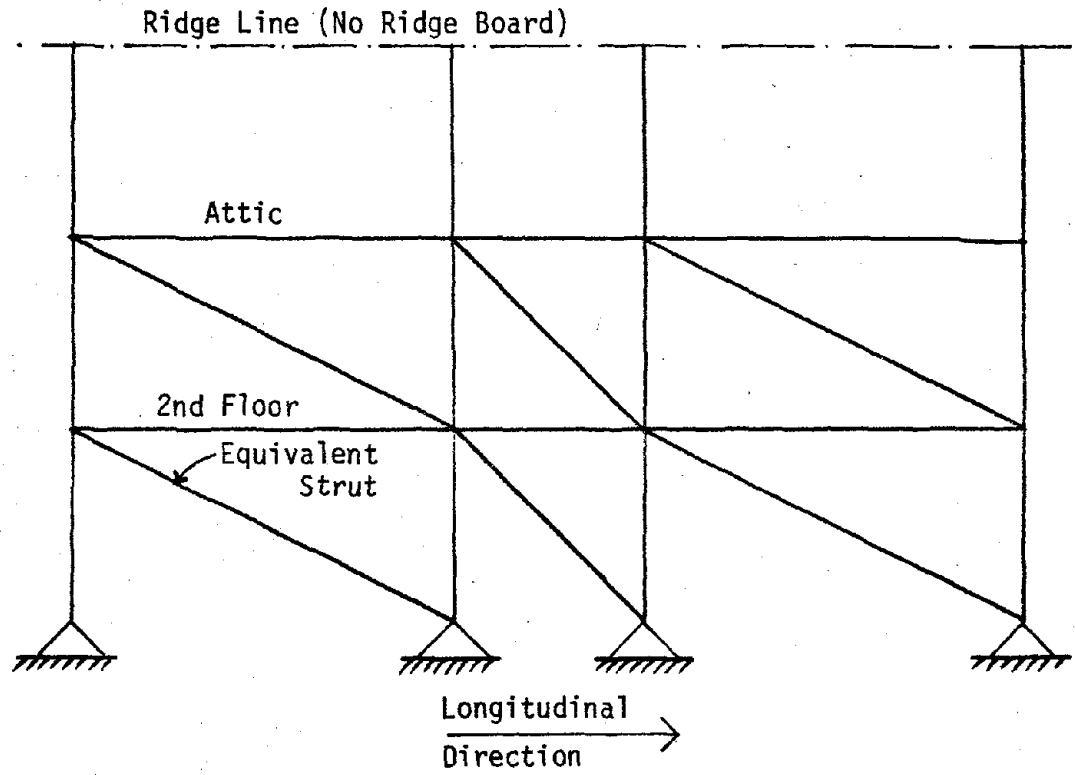


Figure 2.9 Whipple Matthews House
Timber Truss Longitudinal Direction

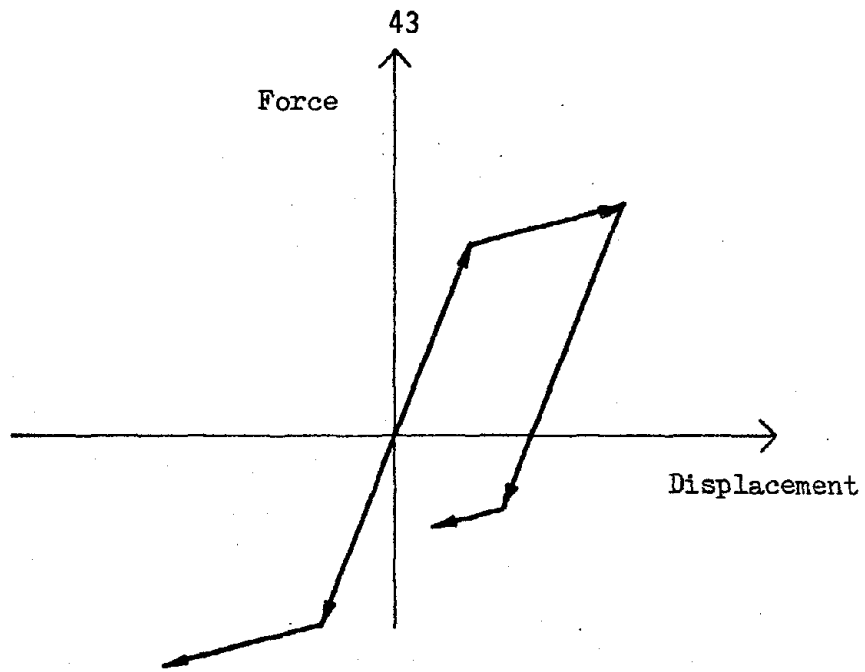


Figure 2.10a Truss Elements
Yield in Tension & Compression

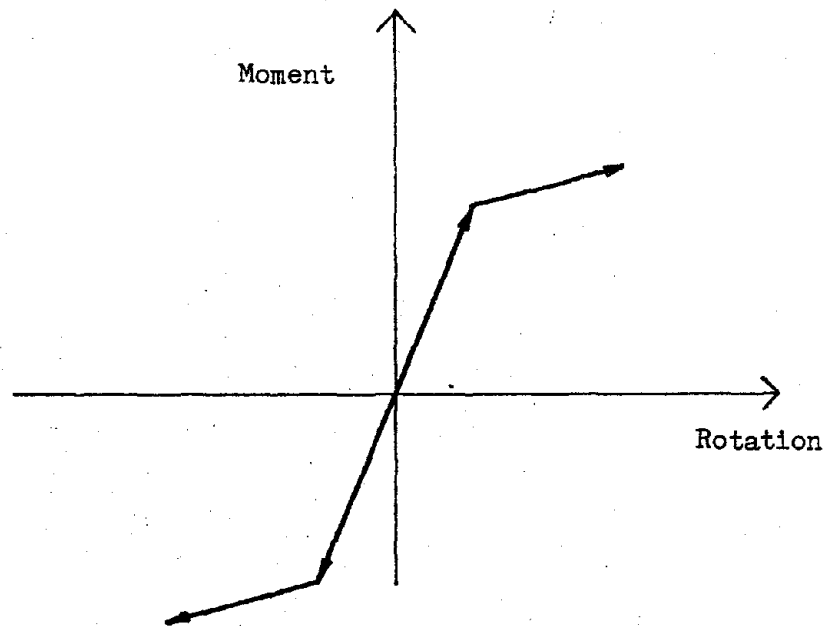


Figure 2.10b Beam Element
Moment Rotation Relationship

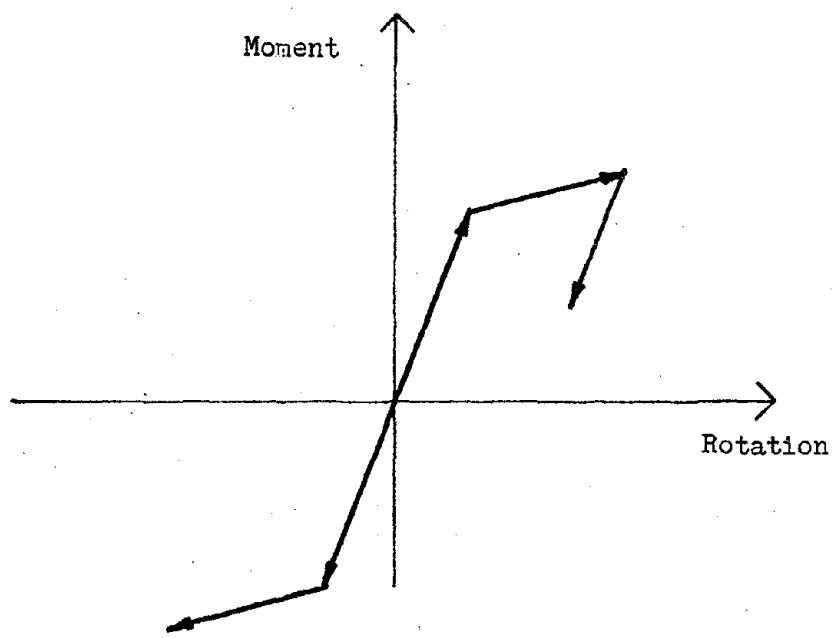


Figure 2.10c Semi-Rigid Connection Element
(Rocking Spring Element)
Moment Rotation Relationship

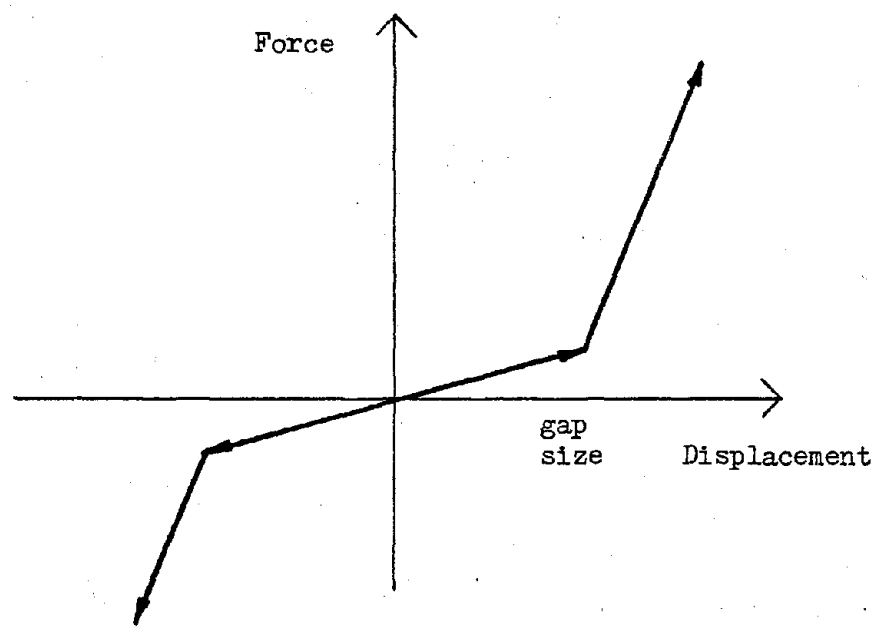


Figure 2.10d Impact Element
(Modified Shear Connection Element)

RESPONSE SPECTRUM

IMPERIAL VALLEY EARTHQUAKE MAY 18, 1940 - 2037 PST

IIIAD01 40.001.0 EL CENTRO SITE IMPERIAL VALLEY IRRIGATION DISTRICT COMP 500E

DAMPING VALUES ARE 0. 2. 5. 10 AND 20 PERCENT OF CRITICAL

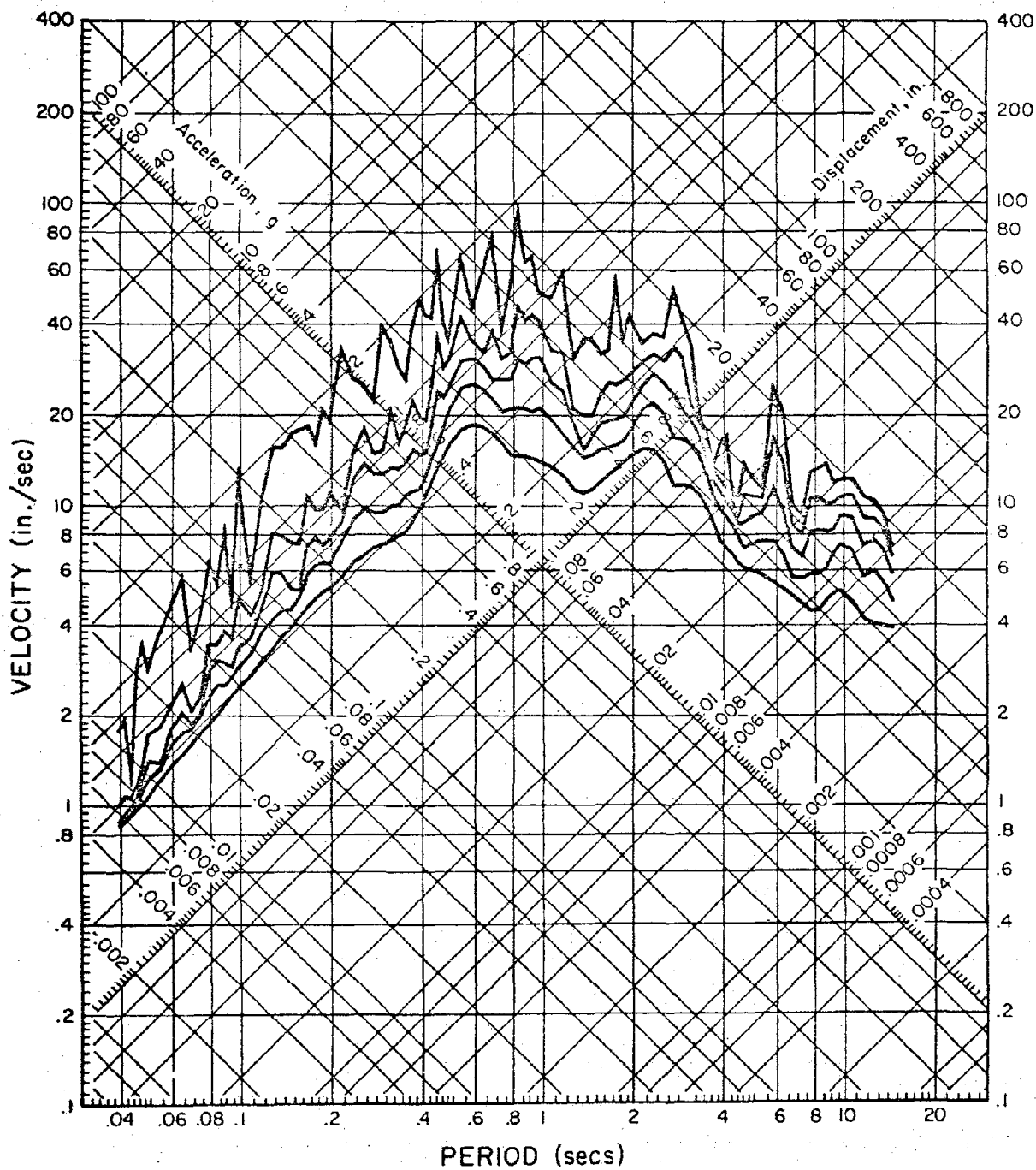


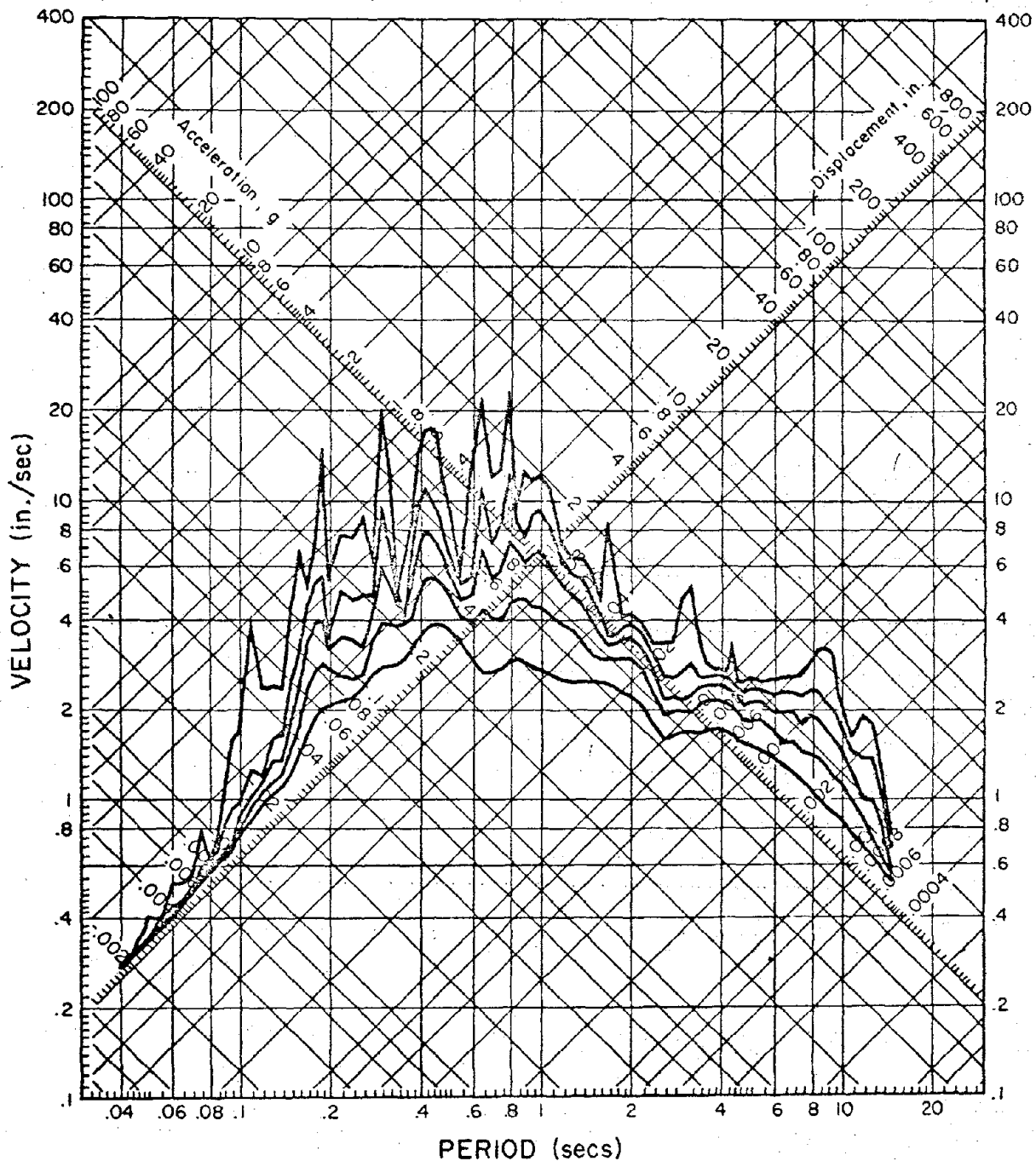
Figure 2.11a

RESPONSE SPECTRUM

NORTHWEST CALIFORNIA EARTHQUAKE OCT 07, 1951 - 2011 PST

111A002 51.001.0 FERDALE CITY HALL COMP N46W

DAMPING VALUES ARE 0, 2, 5, 10 AND 20 PERCENT OF CRITICAL



PERIOD (secs)

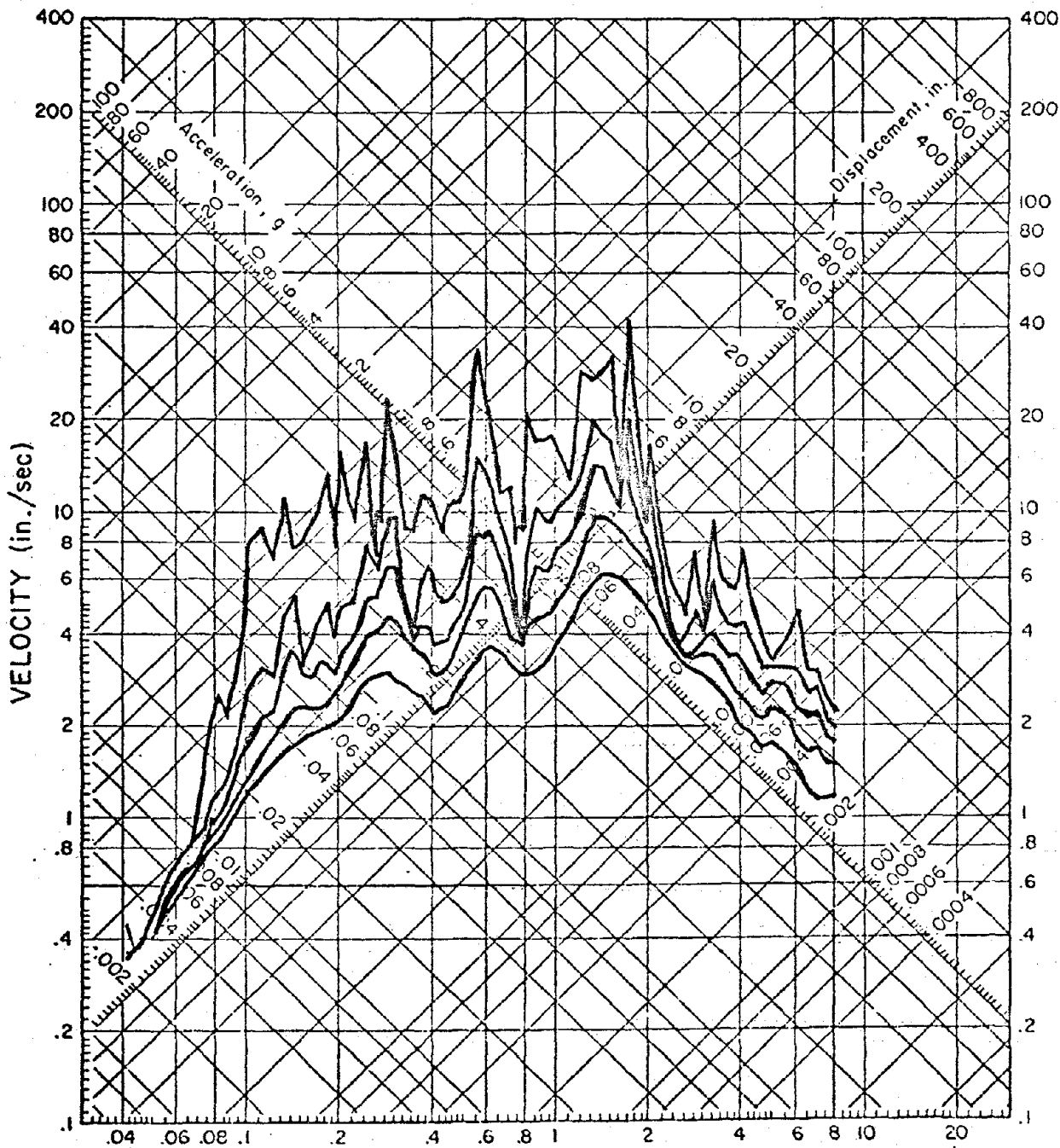
Figure 2.11b

RESPONSE SPECTRUM

SAN FERNANDO EARTHQUAKE FEB 9, 1971 - 0600 PST

IIIG114 71.064.0 PALMDALE FIRE STATION, STORAGE ROOM, PALMDALE, CAL. COMP S30H

DAMPING VALUES ARE 0, 2, 5, 10 AND 20 PERCENT OF CRITICAL



PERIOD (secs)
Figure 2.11c

Table 2.4
Parametric Study Outline

Chimney Parameters.

E=216000 ksf*
E=108000 ksf
E= 54000 ksf
E= 144 ksf
E= 54000 ksf outside/216000 ksf inside

House Parameters.

House Mass due to Wall "A"*
House Mass due to Wall "C"
Chimney House-Connection
Infinitely Rigid Link
Actual Link*
Impact Element
gap = 0.005', 0.1', 0.015', 0.02', 0.04', 0.05'

Ground Parameters

Soil Rocking Spring
Standard * =5580000 ft-kips/rad.
10% Standard =558000 ft-kips/rad.
1% Standard =55800 ft-kips/rad.

Earthquake Motions

Center
Ferndale
Palmdale

* Denotes standard model.

CHAPTER 3 - ANALYSIS RESULTS

3.1 Introduction

The objective of this Chapter is to discuss the results of the free and forced vibration analyses. The discussion compares the standard model, which has basic properties, with the other models in which the chimney, house and ground parameters varied.

3.2 Free Vibration Analysis

The natural frequencies and mode shapes of the various models are shown in Table 3.1 and Figure 3.1. Only the first five modes are shown, because the accuracy of the analytical model and the eigenvalue solution is uncertain in the higher modes.

The fundamental frequency of the standard model is 11.8 Hz. This compares with 13.3 Hz for CASD of the preliminary analysis described in Section 2.2. Although the present model has included the stiffness of the house, which would tend to increase the fundamental frequency, the reduction in the fundamental frequency in the present model is due to the softening effect of the foundation rocking spring.

3.2a Chimney Parameters

In comparing the standard model with the models in which the elastic modulus of the chimney varies, it can be generally stated that the fundamental frequency increases as the modulus increases. The general trend is indicated in the graph of natural fundamental frequency vs. elastic modulus, shown in Figure 3.2. The exception is the case where the modulus is 54,000 ksf above the roofline and 216,000 ksf below the roofline. The frequencies

and mode shapes for this case are essentially the same as for the standard model.

3.2b House Parameters

In comparing the standard model with the models in which the house mass increases, it is observed that the fundamental frequency has decreased.

The frequencies for case 3, where the chimney-house connection has been assumed to be very small, so that the house and chimney behave independently, correspond to that of the house alone and the chimney alone. The first three modes correspond to the three modes of the house, while the next two modes correspond to the first two frequencies of the chimney alone. The fundamental frequency of the chimney mass alone with rocking spring is approximately 18 Hz.

The fundamental frequency for case 4, where the actual sizes of the horizontal timber frame members were used in the assumed rigid chimney-house connection, is smaller than the standard model. This result seems reasonable since the overall structural stiffness has been slightly reduced.

3.2c Ground Parameters

In comparing the standard model with the models where the foundation springs have been reduced, it is observed that the fundamental frequency is drastically reduced. As previously mentioned, the intention here was to determine the foundation rocking spring stiffness at which the house begins to restrain the chimney. It is observed that at 10% of the standard rocking spring stiffness, the fundamental frequency is slightly larger than the fundamental frequency of the house alone.

The corresponding shear wave velocity for the soil would be approximately 273 ft/sec. The fundamental frequency for the case of 1% standard rocking spring is slightly less than that of the house alone. The shear wave velocity for the soil corresponding to this stiffness would be approximately 86 ft/sec. Average soft soil would have a low-strain shear wave velocity of maybe 300 - 400 ft/sec. Due to straining, the effective velocity may be reduced to 1/3 of the above values. Therefore, a shear wave velocity of 273 ft/sec seems low, but 86 ft/sec seems unrealistically low.

Inspection of the higher modes confirms the well known fact that soil-foundation interaction may affect the fundamental mode (Figure 3.1), and frequency of vibration (Table 3.1) appreciably but its effects are small on the second mode frequency and negligible in the higher modes.

3.3 Dynamic Analysis Results

The purpose of performing the dynamic analysis was to determine the force levels and the failure locations in the chimney when subjected to earthquakes. The force results will be discussed in four parts: a) chimney parameters, b) house parameters (except impact), c) ground parameters and d) gap model.

The force results of the various models will be compared with the standard model and a rigid body chimney model, Tables 3.2. The rigid body chimney model assumes that the chimney is very stiff so that the shear force at any location on the chimney may be obtained by multiplying the total mass above that location by 32.2 ft/sec^2 , the scaled peak ground acceleration. The rigid body shear forces are shown in Table 3.2.

In order to understand the general trends of behavior in each of the

various models, the force results for each earthquake were averaged together. These average shears and moments are shown in Tables 3.3a and 3.3b, respectively. Particular attention will be directed toward the portion of the chimney above the roofline because this is where most of the reported damage occurred. The first three elements and the first four nodes correspond to the portion of the chimney above the roofline.

It should be noted that the force results are obtained for a lumped mass system. In particular, the shear force at element 1 (Figure 2.7) is computed due to the lumped mass at node 1, and is constant over the length of the element. The shear force should be adjusted since the chimney is really a distributed mass system, where the shear force would vary linearly over the length. Therefore, tabulated shear forces due to the lumped mass system are approximately the shear force at mid-height of the actual distributed mass system. Although the distributed mass shear forces may slightly affect the earthquake intensity results, the adjustment of the lumped mass results is avoided for simplicity's sake.

3.3a Chimney Parameters

In general, the force levels above the roofline vary only slightly for each variation in the elastic modulus of the chimney. A plot of the elastic modulus vs. the average shear force in element 3, shown in Figure 3.3, depicts this slight variation. The exception is case 10, where the modulus has been reduced to 144 ksf. The forces are significantly smaller than the forces of the standard model, due to the drastic reduction in the chimney stiffness.

Note the slight increase in shear for case 9, where the modulus has

been reduced to 54000 ksf. This slight increase seems to be due to the frequency being in a range of higher spectral acceleration. The structural frequency ω has decreased slightly due to the decrease in elastic modulus, but the chimney is still stiff enough to carry the major portion of the lateral load. When the portion of the chimney above the roofline for cases 1, 7, 8 and 9 are compared to the rigid body case, it is observed that the forces are at least three times the rigid body forces.

This amplification, V/V_{rigid} , the ratio of the shear to the rigid body shear, can be explained by comparing the spectral acceleration of each structure. The rigid body case, which has a high fundamental frequency (low period), would accelerate at the peak ground acceleration, as shown in the response spectra in Figure 2.11. Cases 1, 7, 8 and 9, which have a lower fundamental frequency, are in a range of higher spectral acceleration. It is the higher spectral acceleration that causes the increase in force levels.

3.3b House Parameters (except impact).

There are basically two house parameters that vary: the house mass, and the chimney-house connection. By comparing the standard model with case 2, where the house mass was increased, it is observed that the force levels in the chimney have increased. The elements just below each standard connection have increased considerably. The increases in shear at elements 4, 8 and 9 are primarily due to the additional mass being rigidly attached to the chimney so that the connecting house and chimney masses accelerate together. Note also the increase in shear forces above the chimney. This increase can be attributed to the frequency ratio being in a range of higher amplification.

By comparing the standard model and case 3, where the house connection was made very weak so that the house and chimney would respond independently, it is observed that the force levels above the roofline do not change significantly. Below the roofline, the forces are greater in the standard model due to the house mass being "thrown on" to the chimney by the rigid connection. By comparing case 3, with the rigid body case, it is observed that the dynamic amplification is as large as 3.5 at the top element.

In Case 4, where the actual member sizes were used to model the chimney-house connection, the chimney forces are smaller than the standard model. This is primarily due to less force from the house being transferred through the connection to the chimney.

The two ground parameters investigated are the foundation rocking spring modeling the soil structure interaction, and the ground motions. The forces above the roofline in cases 5 and 6, 10% and 1% standard rocking spring stiffness respectively, are only slightly smaller than the standard model. Below the roofline, cases 5 and 6 have different force levels, but the variation of forces throughout the height of the chimney in both cases is similar. For example, in case 5, elements 1 through 4, the shear increases, then decreases in elements 5 and 7, and then increases again in elements 7 and 8. This peculiar variation in force levels throughout the height of the chimney is due to the higher modes of the house causing some of the lateral load. The contribution of the house to the lateral stiffness becomes possible because of the lower frequency, rigid body rotational mode of the chimney with reduced rocking spring stiffness.

The effects of the individual ground motions on the house-chimney system may be seen in Tables 3.2. The force levels are generally higher for

the Palmdale recording of the San Fernando Earthquake than for the other earthquakes. This is primarily due to the higher spectral values in the short period range of the digitized accelerogram.

3.3c Impact

In the previously discussed models the house and chimney were either completely connected together at each level or not connected at all to behave independently of one another. The mean forces for these cases varied only slightly above the roofline where failure reportedly occurred. The present section deals with the situation where there is a gap between the house and chimney. The modeling of the gap type chimney-house connection was described in Section 2.5, and the time step used for the analysis was explained in Section 2.4.

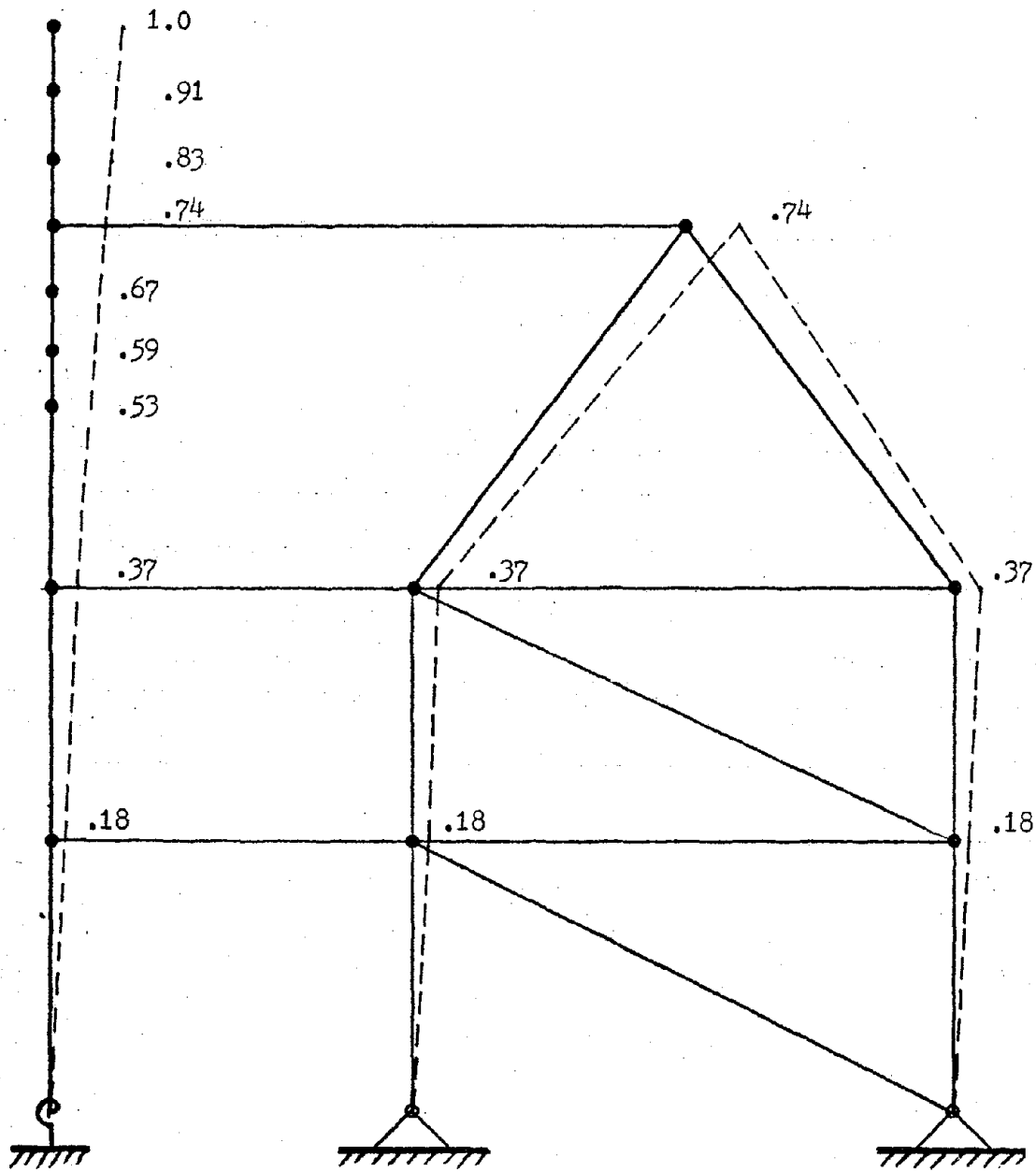
The "average" force results are shown in Tables 3.4. Notice that the shear force at the top node for the .01' gap model has been amplified approximately 15 times that of the rigid body shear forces. From these results it would appear that impact is an important factor in chimney damage. But, it should be remembered that an inelastic analysis has been performed and the results don't have full meaning until the forces and gaps have been scaled down to a realistic level. The scaling procedure commonly used for elasto-plastic analysis is also employed here. The peak ground acceleration, force results and gap size are all scaled by the same factor. As an example, the .01' gap case if scaled down to .10g peak ground acceleration would have 10% of the force results for a gap size of .001'. This gap size is extremely small, but would still produce the same highly amplified forces when compared to the rigid body cases. Therefore the structural integrity

of the chimney-house connection appears to be an important factor in chimney damage. If the connection is either very strong or very weak, the force levels in general do not appear to vary significantly regardless of the variation of the other parameters. But if the connection is similar to the gap modulus, then a potentially damaging situation exists.

MODE	1	2	3	4	5	6	7	8	9	10	HOUSE ALONE	
1	STANDARD MODEL 216000/A/558000	216000/C/558000	216000/A-WEAK LINKS/558000	216000/A-ACTUAL LINKS/ 558000	216000/A/55800	216000/A/5580	54000-216000/A/558000	108000/A/558000	54000/A/558000	144/A/558000	COSD	COSD/558000
2	11.8 (2.3)	10.7 (2.3)	4.9	10.9 (1.9)	5.7 (2.0)	4.3 (2.1)	11.8 (2.3)	10.7 (2.1)	9.8 (1.9)	2.9	32.7 (1.8)	18.4 (3.0)
3	35.6 (1.9)	32. (1.8)	11.9	27. (1.7)	34. (1.6)	34. (1.7)	35. (1.9)	30. (2.0)	22. (2.0)	4.1	73. (1.6)	48.0 (3.5)
4	120. (1.3)	111. (1.3)	17.1	88. (1.7)	119. (1.8)	119. (1.8)	89. (1.3)	74. (1.4)	61. (1.6)	8.	159. (1.1)	149. (1.6)
5	145. (.64)	134. (.8)	18.5	126 (.53)	144. (1.3)	144. (1.3)	135. (.64)	106. (.76)	74. (.92)	11.	229. (.85)	217. (.2)
5	330. (.03)	326. (.01)	1.0	271 (.004)	330. (.002)	330. (.002)	293. (.03)	231. (.002)	165. (.01)	-	364. (.9)	364. (.73)

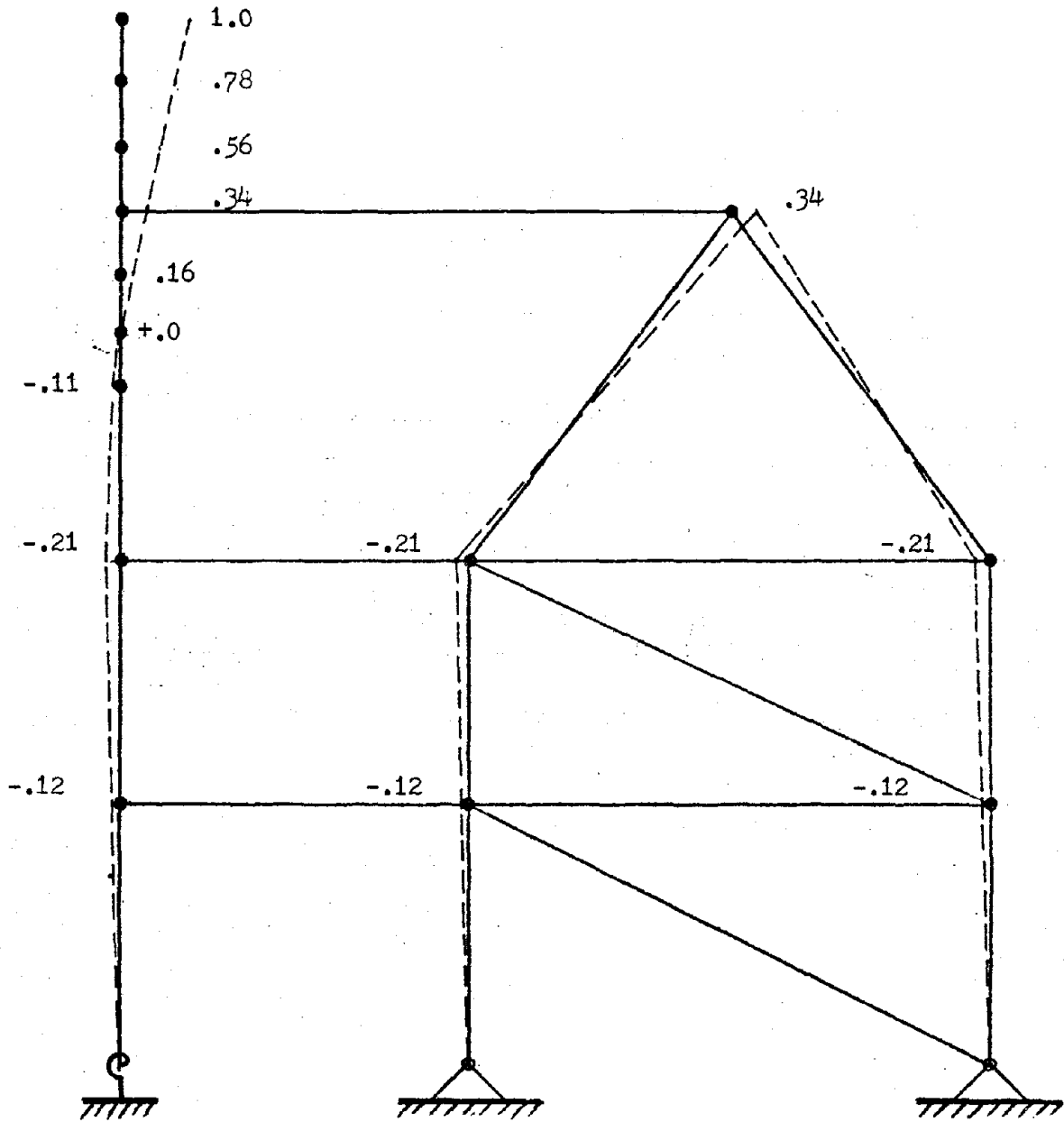
Participation Factors are Shown in ()

Table 3.1 Frequencies



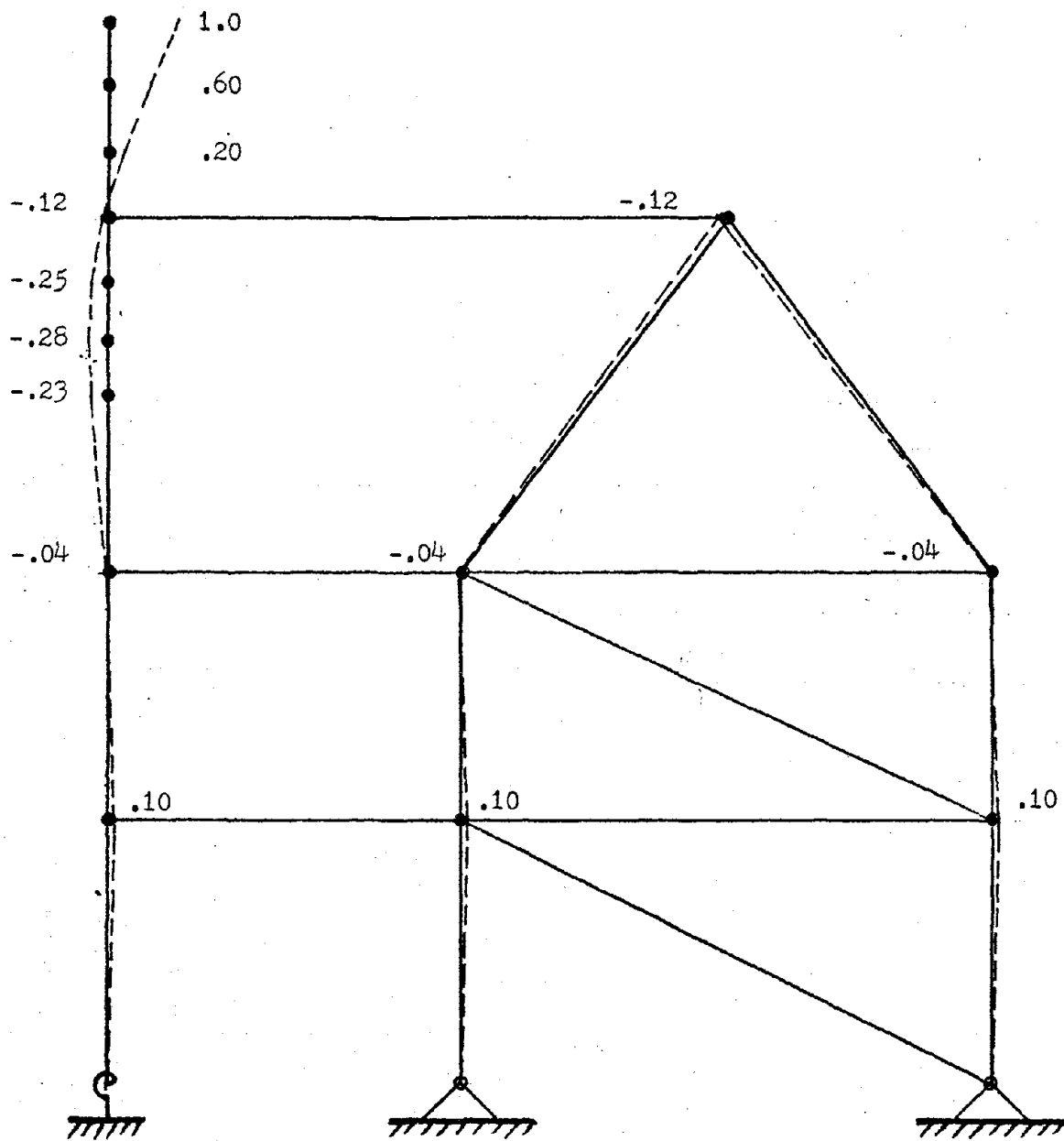
Mode 1
 Frequency= 11.8 Hz
 Participation Factor= 2.3

Figure 3.1a Standard Model Mode Shapes



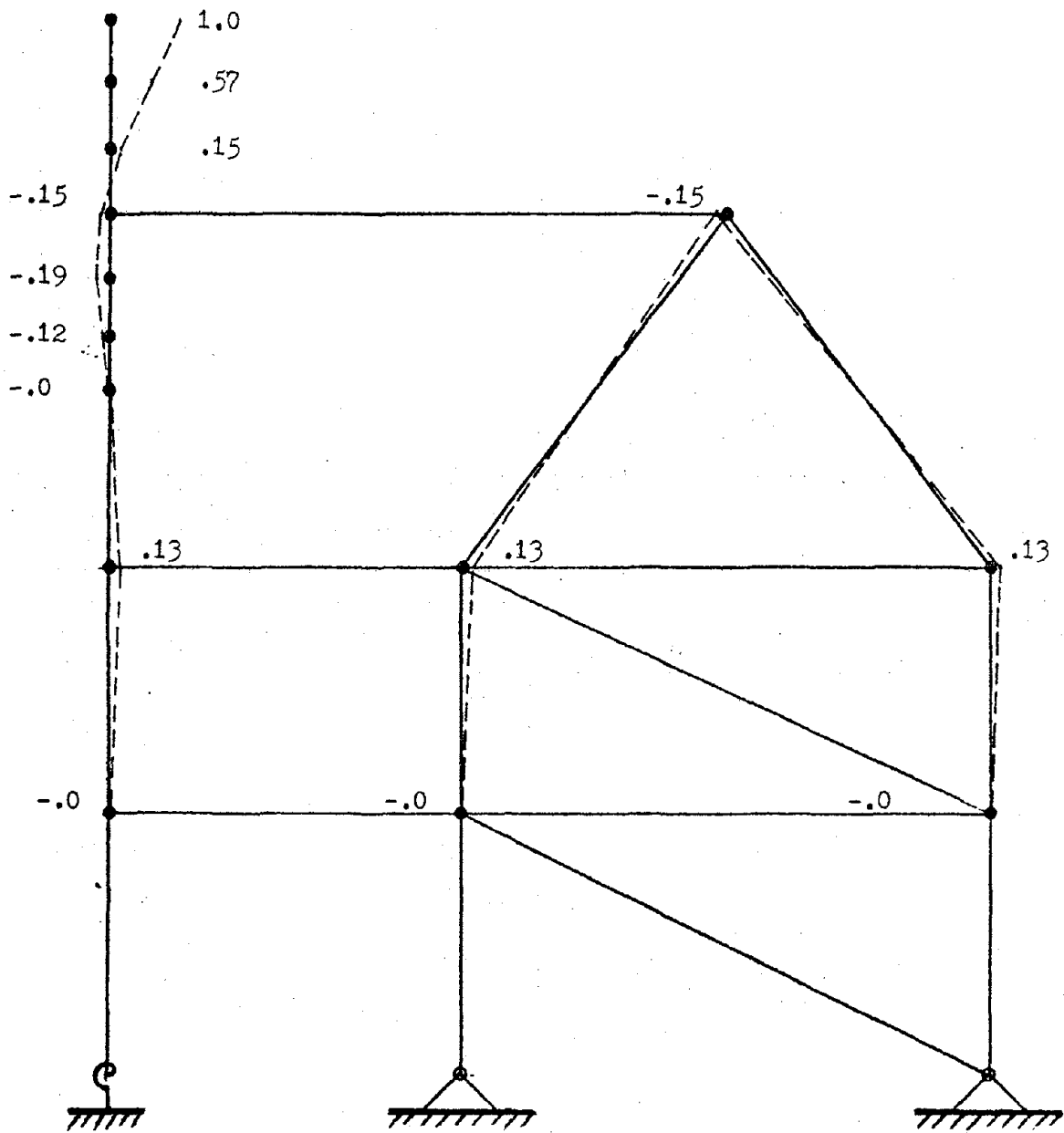
Mode 2
 Frequency= 35.6 Hz.
 Participation Factor= -1.9

Figure 3.1b Standard Model Mode Shapes



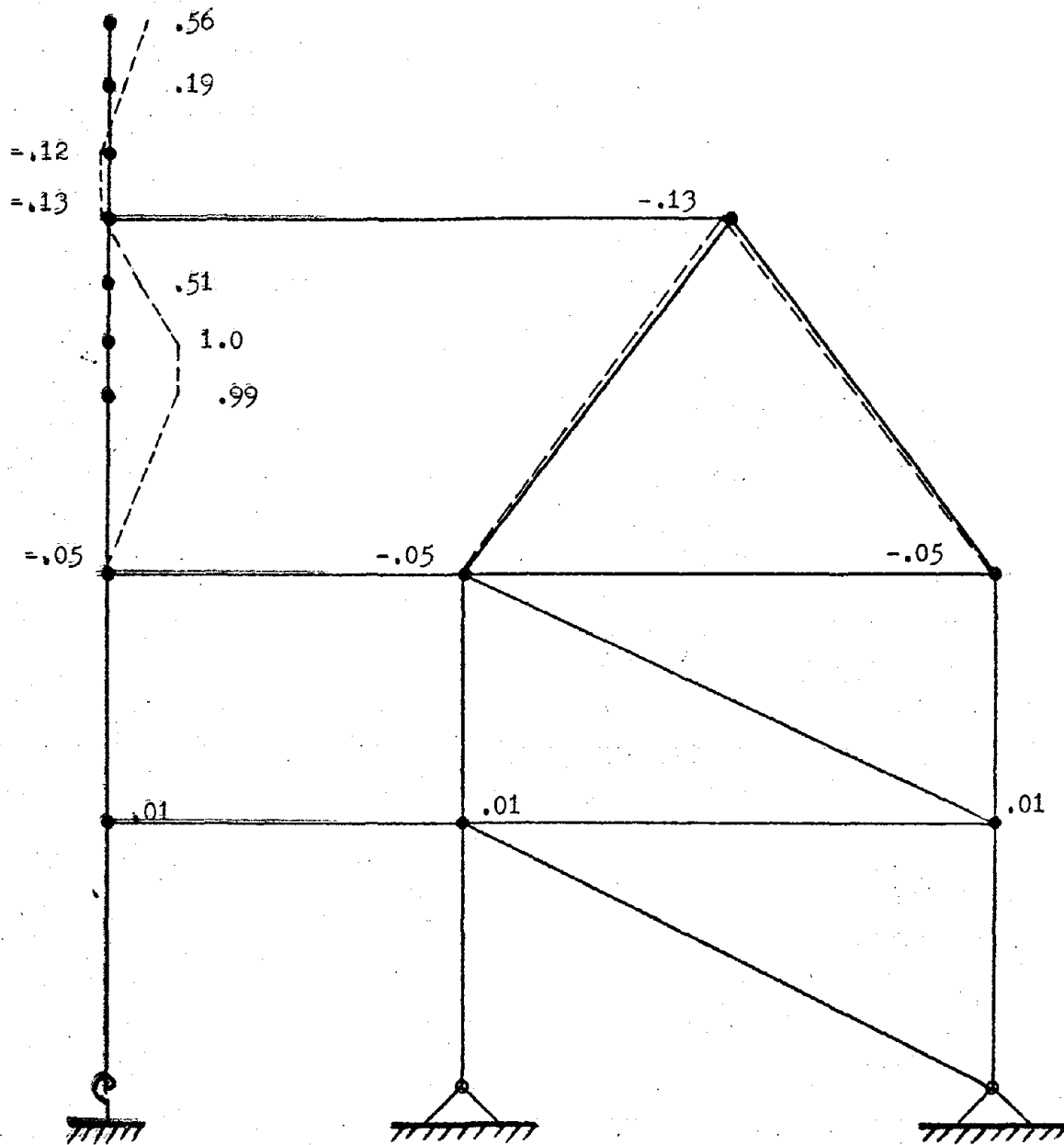
Mode 3
Frequency= 120 Hz.
Participation Factor= 1.3

Figure 3.1c Standard Model Mode Shapes



Mode 4
 Frequency = 145 Hz.
 Participation Factor = -.64

Figure 3.1d Standard Model Mode Shapes



Mode 5
 Frequency= 330 Hz.
 Participation Factor= 0.03

Figure 3.1e Standard Model Mode Shapes

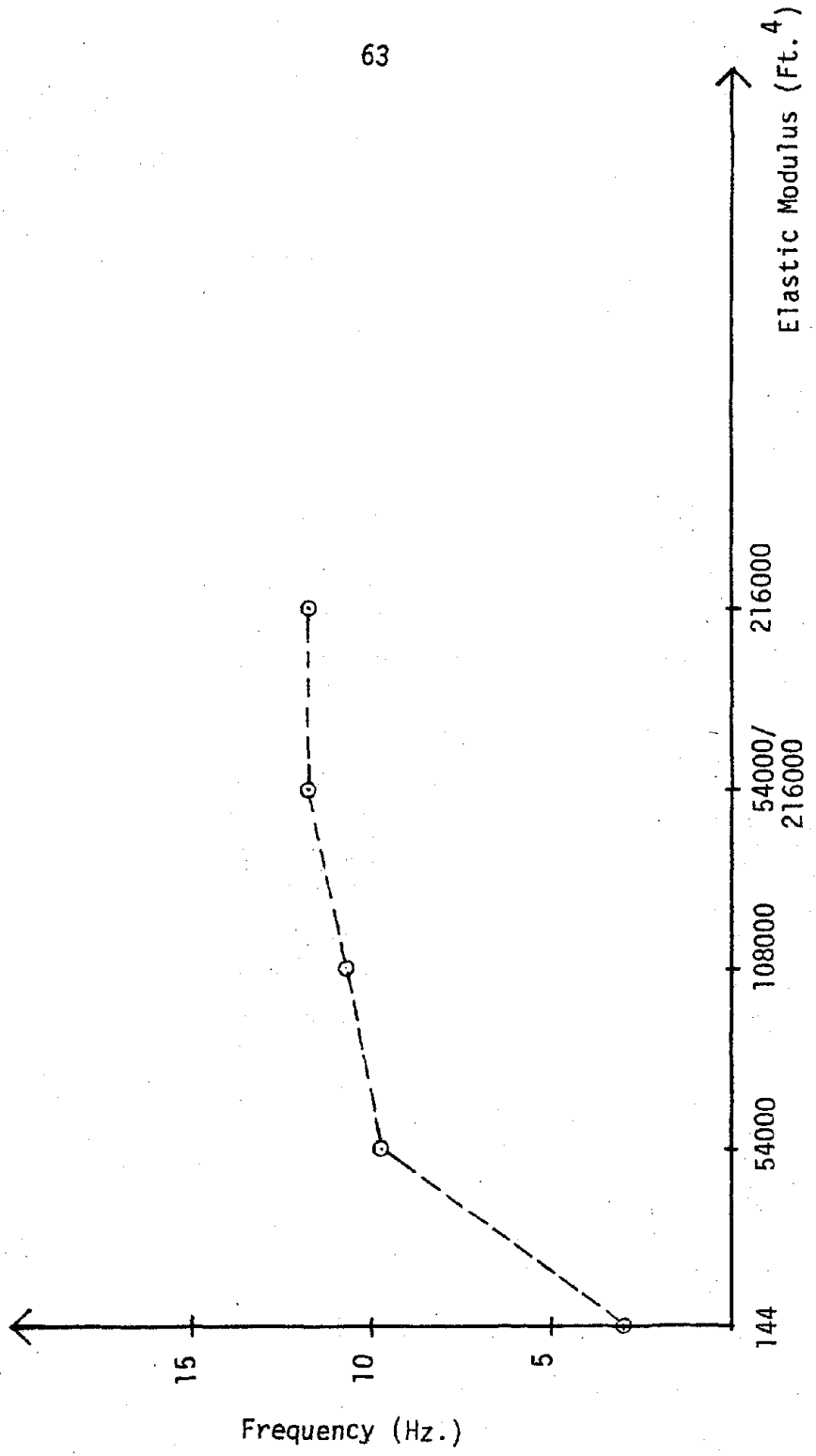


Figure 3.2 Frequency vs. Modulus

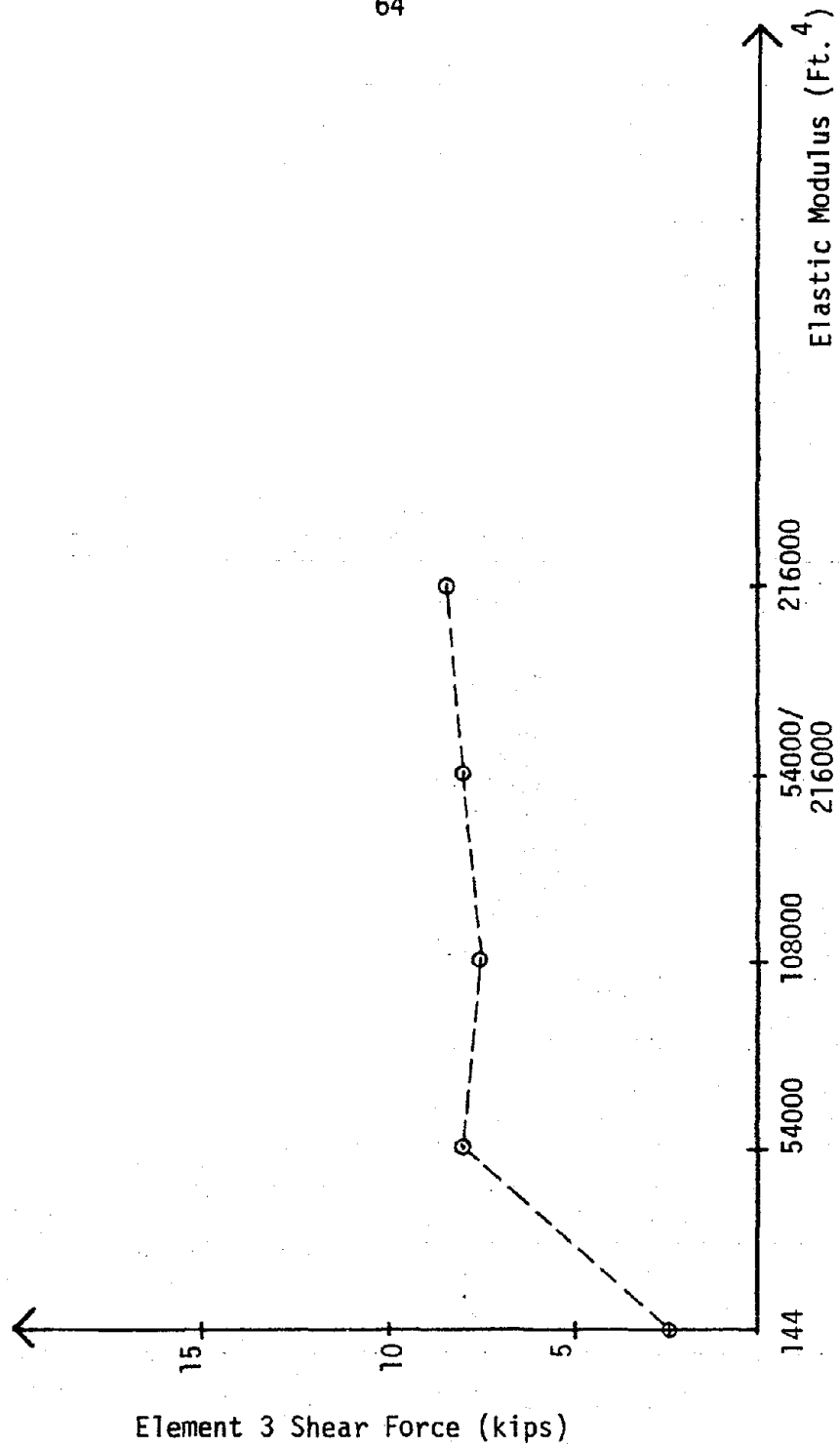


Figure 3.3 Element 3 Shear Force vs. Elastic Modulus

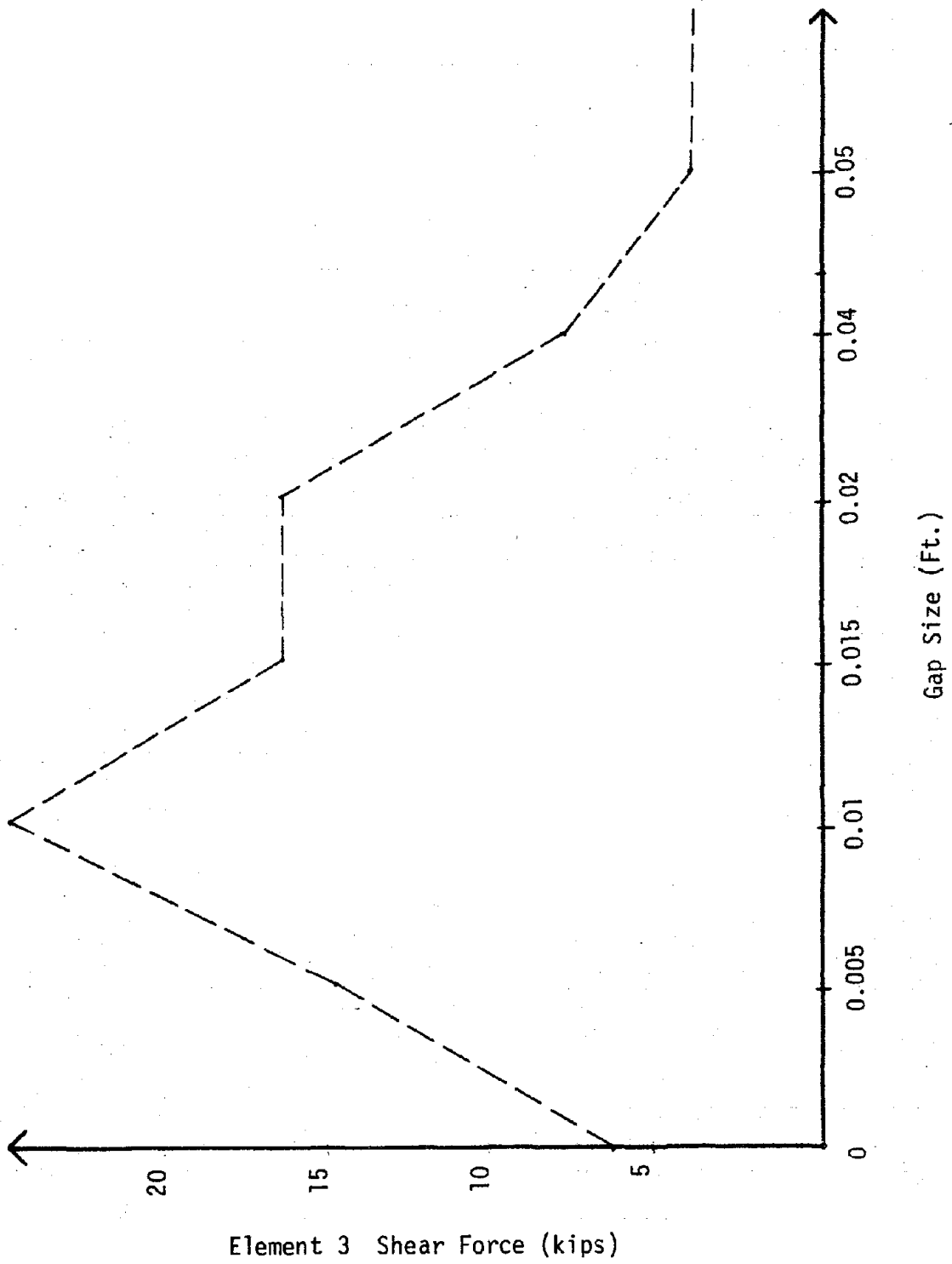


Figure 3.4 Element 3 Shear Force vs. Gap Size

Case 1 2 3 4 5 6 7 8 9 10

Element	1	2	3	4	5	6	7	8	9	10
Standard Model 21600/A/5580000*	1.76 (.22)	1.72 (.22)	1.35 *(.28)	1.24 (.31)	1.57 (.24)	1.45 (.26)	1.89 (.20)	1.72 (.22)	1.99 (.19)	.84 *(.45)
216000/6/5580000	4.94 (.23)	4.75 (.24)	3.75 (.31)	3.52 (.33)	4.38 (.26)	3.92 (.29)	5.22 (.22)	4.77 (.24)	5.37 (.21)	1.95 (.6)
216000/A-Weak Links/5580000	7.87 (.25)	7.37 (.26)	5.86 (.33)	5.61 (.34)	6.86 (.28)	5.98 (.32)	8.11 (.24)	7.46 (.26)	8.16 (.24)	3.15 (.61)
216000/A-Actual Links/5580000	30.04 *(.088)	33.62 *(.079)	7.58 (.35)	24.89 *(.11)	14.97 *(.18)	36.94 *(.071)	29.55 *(.089)	23.17 *(.11)	17.72 *(.15)	5.29 (.50)
	32.10 (.10)	33.34 (.095)	9.02 (.37)	26.47 (.13)	13.97 (.24)	36.01 (.093)	31.54 (.11)	24.93 (.13)	19.57 (.17)	3.18 (4.05)
	33.92 (.12)	36.76 (.11)	10.82 (.37)	27.92 (.14)	12.96 (.31)	35.06 (.12)	33.3 (.12)	26.5 (.15)	21.09 (.19)	1.46 (2.77)
	37.05 (.15)	39.24 (.14)	12.45 (.43)	30.53 (.18)	12.75 (.42)	33.19 (.16)	36.33 (.15)	28.99 (.19)	23.57 (.23)	5.12 (1.05)
	103.84 (.18)	121.92 (.15)	32.4 (.57)	95.19 (.19)	55.24 (.33)	21.34 (.86)	102.58 (.18)	90.97 (.20)	84.30 (.21)	2.58 (7.15)
	169.25 (.26)	219.51 (.20)	66.31 (.68)	156.91 (.29)	117.71 (.38)	65.46 (.68)	169.13 (.26)	160.01 (.28)	144.45 (.31)	19.15 (2.34)
Rigid Body Shear										.55
										1.64
										2.74
										3.78
										4.78
										5.77
										7.77
										26.35
										64.0

Table 3.2a Shear Envelope Values (E1 Centro)

Case	1	2	3	4	5	6	7	8	9	10
Element	Standard Model 21600/A/5580000	216000/6/5580000	216000/A-Weak Links/5580000	216000/A-Actual Links/5580000	216000/A/558000	216000/A/55800	54000-216000/A/ 5580000	108000/A/5580000	54000/A/5580000	144/A/5580000
2	3.16 (.15)	3.1 (.15)	2.43 (.19)	2.23 (.21)	2.82 (.16)	2.61 (.13)	3.41 (.13)	3.09 (.15)	3.58 (.13)	1.51 (.30)
3	12.06 (.12)	11.66 (.12)	9.19 (.15)	8.56 (.16)	10.7 (.13)	9.68 (.15)	12.81 (.11)	11.67 (.12)	13.24 (.15)	4.77 (.29)
4	26.10 (.089)	24.93 (.093)	19.73 (.12)	18.66 (.12)	23.04 (.10)	20.44 (.11)	27.41 (.085)	25.11 (.093)	27.92 (.083)	10.34 *(.23)
5	74.17 (.043)	78.72 (.041)	31.55 (.10)	58.48 (.055)	27.29 (.12)	51.93 (.062)	14.68 (.043)	62.18 (.051)	55.58 (.058)	6.82 (.47)
6	125.53 (.032)	135.27 (.030)	46.29 (.088)	100.83 (.040)	46.38 (.088)	103.75 (.037)	125.15 (.032)	102.15 (.04)	86.69 (.047)	8.88 (.46)
7	179.80 (.027)	194.14 (.025)	62.73 (.078)	145.51 (.034)	66.06 (.074)	164.53 (.030)	178.43 (.027)	144.55 (.034)	120.64 (.041)	8.31 (.6)
8	357.62 *(.018)	382.48 *(.017)	122.48 *(.053)	292.067 *(.022)	127.25 (.051)	323.55 *(.020)	352.82 *(.019)	283.70 *(.023)	233.76 (.028)	16.38 (.4)
9	1084.51 (.021)	1160.91 (.019)	335.43 (.067)	958.37 (.023)	390.58 (.057)	325.70 (.069)	1070.89 (.021)	887.81 (.025)	819.89 *(.027)	16.6 (1.35)
10	2307.67 (.024)	2684.95 (.02)	823.27 (.066)	2131.06 (.026)	127.3 *(.045)	180.77 (.30)	2308.15 (.024)	2058.61 (.026)	1868.93 (.029)	137.55 (.39)

Table 3.2b Moment Ending Values (EI Centro)

Case	1	2	3	4	5	6	7	8	9	10
Element	Standard Model 216000/6/5580000	216000/6/5580000	216000/A-Weak Links/5580000	216000/A-Actual Links/5580000	216000/A/558000	216/A/55800	54000-216000/A/ 5580000	108000/A/5580000	54000/A/5580000	144/A/5580000
1	3.39 (.11)	4.50 (.084)	3.83 *(.099)	2.44 (.16)	2.43 (.16)	2.40 (.16)	3.25 (.12)	3.13 (.12)	3.35 (.11)	.45 *(.84)
2	9.04 (.13)	11.86 (.097)	10.26 (.11)	6.6 (.17)	6.25 (.19)	6.20 (.19)	8.32 (.14)	7.96 (.14)	8.36 (.14)	.89 (1.29)
3	13.58 (.14)	17.57 (.11)	15.49 (.12)	10.24 (.19)	9.09 (.21)	9.01 (.21)	12.52 (.15)	11.37 (.17)	11.85 (.16)	1.15 (1.67)
4	49.36 *(.053)	78.55 *(.034)	19.34 (.14)	28.34 *(.093)	33.73 *(.078)	33.9 *(.078)	46.08 *(.057)	34.15 *(.077)	24.30 *(.11)	2.18 (1.21)
5	52.16 (.064)	80.98 (.041)	22.16 (.15)	28.79 (.12)	34.7 (.096)	34.71 (.096)	48.31 (.069)	35.60 (.094)	25.64 (.13)	1.25 (2.67)
6	53.72 (.075)	82.40 (.049)	24.57 (.16)	29.77 (.14)	35.0 (.12)	34.90 (.12)	49.90 (.081)	36.27 (.11)	26.31 (.15)	.59 (6.85)
7	55.70 (.097)	83.98 (.064)	28.54 (.19)	31.24 (.17)	34.64 (.16)	34.47 (.16)	52.04 (.10)	36.43 (.15)	26.74 (.20)	2.47 (2.19)
8	94.05 (.2)	92.32 (.2)	58.61 (.32)	67.43 (.27)	24.5 (.75)	12.78 (1.44)	92.05 (.20)	83.41 (.22)	60.26 (.31)	1.22 (15.12)
9	146.49 (.31)	182.62 (.25)	100.95 (.44)	96.46 (.46)	57.46 (.78)	49.81 (.9)	144.50 (.31)	127.31 (.35)	107.53 (.42)	6.16 (7.28)

Table 3.2c Shear Envelope Values (Palm Dale)

Case	1	2	3	4	5	6	7	8	9	10
Element	Standard Model 216000/A/5580000	216000/6/5580000	216000/A-Weak Links/5580000	216000/A-Actual Links/5580000	216000/A/5580000	216000/A/55800	54000-216000/A/ 5580000	108000/A/5580000	54000/A/5580000	144/A/5580000
2	6.10 (.075)	8.10 (.057)	6.89 (.067)	4.40 (.10)	4.37 (.11)	4.31 (.11)	5.84 (.079)	5.63 (.082)	6.02 (.076)	.82 (.56)
3	22.37 (.062)	29.44 (.047)	25.36 (.055)	16.17 (.086)	15.63 (.089)	15.47 (.09)	20.81 (.067)	19.96 (.07)	21.01 (.066)	2.39 (.58)
4	46.81 (.05)	61.06 (.038)	53.24 (.044)	34.61 (.067)	31.97 (.073)	31.69 (.074)	43.13 (.054)	40.43 (.058)	42.34 (.055)	4.2 (.55)
5	126.59 (.025)	186.74 (.077)	84.18 (.038)	66.88 (.048)	85.72 (.037)	84.34 (.038)	116.85 (.027)	91.27 (.035)	78.91 (.041)	2.48 (1.29)
6	210.04 (.015)	316.31 (.010)	119.64 (.027)	111.87 (.029)	141.25 (.023)	139.52 (.023)	194.14 (.016)	148.22 (.022)	118.26 (.027)	3.9 (8.21)
7	296.0 (.0166)	447.98 (.011)	158.43 (.031)	159.5 (.031)	197.26 (.025)	195.18 (.025)	273.98 (.018)	206.25 (.024)	160.36 (.031)	3.72 (1.32)
8	563.38 *(.012)	848.76 *(.0077)	291.74 *(.022)	309.45 *(.021)	363.52 *(.018)	360.63 *(.018)	523.77 *(.013)	381.11 *(.017)	288.73 *(.023)	8.13 (.81)
9	1068.54 (.021)	1392.91 (.016)	693.77 (.032)	781.5 (.029)	369.13 (.061)	366.06 (.061)	1041.80 (.022)	758.38 (.03)	515.61 (.043)	6.54 (9.43)
10	1894.91 (.029)	1850.08 (.029)	1353.24 (.040)	1348.93 (.040)	470.77 (.12)	61.79 (.88)	1882.43 (.029)	1633.88 (.033)	1097.56 (.05)	45.99 (1.18)

Table 3.2d Moment Envelope Values (Palm Dale)

Case	1	2	3	4	5	6	7	8	9	10
Element	216000/A/5580000	216000/6/5580000	216000/A-Weak Links/ 5580000	216000/A-Actual Links/5580000	216000/A/5580000	216000/A/55800	54000-216000/A/ 5580000	108000/A/5580000	54000/A/5580000	144/A/5580000
1	.67 (.58)	.76 (.5)	*.62 (.61)	.75 (.51)	1.14 (.33)	1.081 (.35)	.69 (.55)	.82 (.46)	.84 (.45)	*.74 (.51)
2	1.98 (.58)	2.23 (.52)	1.81 (.64)	2.12 (.54)	3.33 (.35)	3.40 (.37)	1.97 (.58)	2.29 (.50)	2.37 (.49)	1.94 (.59)
3	3.25 (.59)	3.58 (.54)	2.98 (.64)	3.35 (.57)	5.43 (.35)	4.00 (.38)	3.22 (.6)	3.59 (.53)	3.83 (.50)	3.07 (.63)
4	*11.64 (.23)	*17.31 (.15)	4.06 (.65)	*14.53 (.18)	*15.64 (.17)	*36.04 (.073)	11.63 (.23)	*10.94 (.24)	8.07 (.33)	4.91 (.54)
5	12.73 (.26)	18.36 (.18)	5.06 (.66)	15.43 (.22)	14.14 (.24)	35.0 (.095)	12.71 (.26)	12.00 (.28)	9.12 (.37)	3.13 (1.07)
6	13.79 (.29)	19.34 (.21)	6.05 (.67)	16.25 (.25)	12.67 (.32)	33.94 (.12)	13.76 (.24)	12.98 (.31)	10.08 (.40)	1.54 (2.62)
7	15.82 (.34)	21.12 (.26)	7.95 (.68)	17.91 (.30)	10.14 (.53)	32.14 (.17)	15.76 (.34)	14.73 (.37)	11.79 (.46)	3.73 (1.45)
8	71.07 (.26)	84.09 (.22)	25.65 (.72)	69.37 (.27)	57.31 (.32)	14.06 (1.31)	71.18 (.26)	67.09 (.28)	73.14 (.25)	1.90 (9.7)
9	148.78 (.30)	188.40 (.24)	60.88 (.74)	127.61 (.33)	138.90 (.32)	63.06 (.71)	149.12 (.30)	144.70 (.31)	156.43 (.29)	19.65 (2.28)

Table 3.2e Shear Envelope Values (Ferdale)

Case	1	2	3	4	5	6	7	8	9	10
Element	Standard Model 216000/A/5580000	216000/6/5580000	216000/A-Weak Links/ 5580000	216000/A-Actual Links/5580000	216000/A/558000	216/A/55800	54000-216000/A/ 5580000	108/A/5580000	54000/A/5580000	144/A/5580000
2	1.21 (.38)	1.40 (.33)	1.11 (.41)	1.36 (.34)	2.05 (.22)	1.94 (.24)	1.24 (.37)	1.47 (.31)	1.51 (.30)	1.33 (.35)
3	4.77 (.29)	5.41 (.26)	4.38 (.32)	5.17 (.27)	8.05 (.17)	7.53 (.18)	4.75 (.29)	5.59 (.25)	5.78 (.24)	4.79 (.29)
4	10.61 (.22)	11.84 (.2)	9.74 * (.24)	11.20 (.21)	17.81 (.13)	16.5 (.14)	10.54 (.22)	12.06 (.19)	12.65 (.18)	10.18 * (.23)
5	29.24 (.11)	39.53 (.081)	16.23 (.2)	34.45 (.093)	15.10 (.21)	49.0 (.065)	29.01 (.11)	28.80 (.11)	25.32 (.13)	6.73 (.48)
6	49.61 (.081)	68.91 (.059)	24.33 (.17)	59.13 (.068)	33.99 (.12)	104.86 (.039)	49.34 (.082)	47.96 (.085)	39.91 (.10)	6.54 (.62)
7	71.68 (.068)	99.86 (.049)	34.01 (.14)	85.13 (.058)	54.2 (.090)	159.16 (.031)	71.36 (.069)	68.73 (.071)	56.05 (.087)	5.84 (.84)
8	147.60 (.044)	201.25 (.033)	72.15 (.091)	170.11 (.039)	102.53 (.063)	311.98 (.021)	146.99 (.044)	139.42 (.047)	112.62 (.058)	12.39 (.53)
9	641.48 (.035)	745.71 (.030)	351.68 (.089)	649.68 (.034)	329.04 (.068)	301.42 (.074)	639.88 (.035)	573.10 (.039)	611.12 (.037)	9.09 (2.65)
10	1754.9 * (.031)	2157.56 * (.025)	706.49 * (.077)	1676.28 * (.032)	1353.89 * (.040)	209.52 (.26)	1756.06 * (.031)	1652.90 * (.033)	1783.97 * (.031)	146.01 (.37)

Table 3.2f Moment Envelope Values (Ferndale)

Element	Impact .003	Impact .005	Impact .01	Impact .015	Impact .02	Impact .03	Impact .04	Impact .05	Impact .40
1	4.13 (.092)	4.99 (.076)*	15.38 (.025)	3.87 (.098)	4.12 (.092)*	2.82 (.13)	1.52 (.25)	1.21 (.31)	.12 (.31)
2	9.18 (.93)	12.95 (.089)	29.91 (.038)	10.07 (.11)	10.35 (.11)	7.46 (.15)	3.95 (.29)	3.42 (.34)	.34 (.34)
3	12.89 (.15)	17.53 (.11)	38.83 (.049)	15.61 (.12)	15.48 (.12)	11.50 (.17)	5.91 (.32)	5.43 (.53)	.54 (.53)
4	27.97 (.070)*	27.63 (.10)	50.29 (.052)	28.94 (.091)*	26.89 (.098)	29.39 (.09)*	22.46 (.12)*	11.04 (.24)*	1.10 (.24)*
5	30.09 (.11)	30.41 (.11)	48.21 (.07)	31.54 (.11)	30.98 (.11)	29.72 (.11)	23.76 (.14)	12.26 (.27)	1.23 (.27)
6	31.07 (.13)	32.73 (.12)	51.81 (.078)	35.60 (.11)	34.52 (.11)	29.82 (.14)	24.52 (.16)	13.39 (.30)	1.34 (.30)
7	35.02 (.15)	37.48 (.14)	52.59 (.10)	41.26 (.13)	39.62 (.14)	32.70 (.17)	26.29 (.21)	15.41 (.35)	1.54 (.35)
8	105.85 (.17)	111.09 (.17)	122.43 (.15)	112.26 (.16)	105.01 (.18)	82.12 (.22)	43.82 (.42)	34.95 (.53)	34.9 (.53)
9	179.19 (.25)	182.82 (.25)	212.16 (.21)	176.36 (.25)	158.07 (.28)	126.36 (.35)	73.17 (.61)	73.17 (.61)	7.31 (.61)

Table 3.2g Shear Envelope Values
216000/A-Actual Links/5580000 - 1.0g El Centro

Element	Impact .003	Impact .005	Impact .01	Impact .015	Impact .02	Impact .03	Impact .04	Impact .05	Impact .40
2	7.43 (.062)	8.99 (.051)	27.69 (.017)	6.97 (.066)	7.41 (.062)	5.07 (.080)	2.73 (.17)	2.18 (.21)	.22 (.21)
3	23.31 (.060)	31.81 (.044)	81.53 (.017)	25.10 (.055)	26.03 (.053)	18.51 (.075)	9.72 (.14)	8.34 (.17)	.83 (.17)
4	46.23 (.050)	63.37 (.037)	146.75 (.016)	52.36 (.044)	53.60 (.043)	39.20 (.059)	19.94 (.12)	18.11 (.13)	1.81 (.13)
5	88.90 (.036)	95.55 (.033)	184.78 (.017)	93.22 (.033)	95.43 (.034)	75.83 (.042)	55.76 (.057)	32.51 (.098)	3.25 (.098)
6	135.52 (.030)	144.21 (.028)	255.83 (.016)	141.24 (.029)	142.72 (.028)	117.66 (.035)	93.08 (.044)	52.10 (.078)	5.21 (.078)
7	183.49 (.027)	196.09 (.025)	320.49 (.015)	198.14 (.025)	196.41 (.025)	163.48 (.030)	131.36 (.037)	73.51 (.067)	7.35 (.067)
8	339.50 (.019)*	368.47 (.018)*	522.09 (.013)*	394.12 (.017)*	383.14 (.017)*	319.89 (.020)*	256.35 (.026)*	147.34 (.044)*	14.73 (.044)*
9	1029.66 (.022)	1086.68 (.021)	1288.97 (.017)	1141.98 (.020)	1093.72 (.020)	855.47 (.026)	545.0 (.041)	391.98 (.057)	39.19 (.057)
10	2305.61 (.024)	2389.86 (.023)	2568.69 (.021)	2439.58 (.022)	2252.37 (.024)	1787.09 (.030)	1032.44 (.053)	890.09 (.061)	88.98 (.061)

Table 3.2h Moment Envelope Values
216000/A-Actual Links/5580000 - 1.0g El Centro

Element	Impact .005	Impact .01	Impact .015	Impact .02	Impact .04	Impact .05	Impact .01
1	3.06 (.12)	3.74 (.10)*	2.85 (.13)	3.61 (.11)	2.15 (.18)	.94 (.40)	.05 (.76)
2	7.39 (.16)	9.83 (.12)	7.08 (.16)	9.21 (.12)	5.17 (.22)	2.42 (.48)	.18 (.64)
3	11.87 (.16)	14.29 (.13)	10.89 (.18)	14.53 (.13)	8.71 (.22)	3.65 (.53)	.30 (.64)
4	23.03 (.11)*	25.13 (.11)	29.82 (.089)*	31.11 (.085)*	27.26 (.097)*	13.69 (.19)*	.94 (.28)*
5	23.63 (.14)	27.23 (.12)	32.23 (.10)	34.91 (.096)	27.62 (.12)	14.51 (.23)	1.02 (.33)
6	24.17 (.17)	29.15 (.14)	34.73 (.12)	37.84 (.11)	27.95 (.14)	15.26 (.26)	1.11 (.37)
7	26.57 (.20)	34.37 (.16)	39.36 (.14)	43.63 (.12)	29.90 (.18)	16.33 (.33)	1.29 (.42)
8	81.70 (.23)	95.23 (.19)	115.80 (.16)	123.88 (.15)	66.59 (.28)	34.57 (.53)	3.48 (.53)
9	143.22 (.31)	160.35 (.28)	186.51 (.24)	188.64 (.24)	114.73 (.39)	71.93 (.62)	7.24 (.62)

Table 3.2i Shear Envelope Values
21600/A - Actual Links/5580000 - 1.0g Ferndale

Element	Impact .005	Impact .01	Impact .015	Impact .02	Impact .04	Impact .05	Impact .01
2	5.51 (.083)	6.73 (.068)	5.13 (.090)	6.49 (.071)	3.88 (.12)	1.69 (.27)	.11 (.42)
3	18.60 (.075)	24.42 (.057)	17.75 (.078)	23.06 (.060)	14.02 (.099)	6.01 (.23)	.43 (.32)
4	39.12 (.060)	50.07 (.047)	36.47 (.064)	48.26 (.048)	29.70 (.078)	12.38 (.19)	.97 (.24)
5	66.35 (.048)	84.35 (.038)	75.37 (.042)	97.76 (.033)	59.54 (.054)	31.97 (.10)	2.38 (.13)
6	98.99 (.041)	122.88 (.033)	126.48 (.032)	153.10 (.027)	102.25 (.040)	53.55 (.076)	3.97 (.10)
7	135.66 (.036)	165.72 (.030)	179.08 (.027)	213.40 (.023)	146.30 (.033)	77.57 (.063)	5.74 (.085)
8	263.21 (.025)*	321.02 (.020)*	364.97 (.018)*	420.08 (.016)*	285.13 (.023)*	155.94 (.042)*	11.88 (.055)
9	826.76 (.027)	976.28 (.023)	1162.48 (.019)	1280.52 (.018)	298.28 (.075)	380.70 (.059)	36.26 (.062)
10	1828.45 (.030)	2144.44 (.025)	2521.10 (.022)	2667.88 (.020)	1534.43 (.035)	897.98 (.061)	90.44 (.060)

Tables 3.2j Moment Envelope Values
21600/A-Actual Links/5580000 - 1.0g Ferndale

Element	Impact .005	Impact .01	Impact .015	Impact .02	Impact .04	Impact .05
1	5.53 (.069)*	6.55 (.058)*	7.22 (.053)*	5.58 (.068)*	2.42 (.16)	172 (.53)
2	13.32 (.086)	15.83 (.073)	16.13 (.071)	13.97 (.082)	5.88 (.20)	2.10 (.55)
3	20.09 (.096)	22.64 (.085)	23.51 (.082)	19.80 (.097)	9.13 (.21)	3.43 (.56)
4	34.35 (.077)	38.56 (.068)	33.13 (.080)	33.41 (.079)	23.47 (.11)*	7.80 (.34)*
5	36.58 (.091)	40.60 (.082)	38.16 (.088)	34.19 (.098)	23.53 (.14)	8.59 (.39)
6	38.47 (.11)	42.70 (.095)	42.62 (.095)	36.16 (.11)	22.96 (.18)	9.39 (.43)
7	44.48 (.12)	48.84 (.11)	48.82 (.11)	42.31 (.13)	21.39 (.25)	10.96 (.49)
8	129.90 (.14)	141.58 (.13)	133.81 (.14)	111.97 (.16)	36.54 (.50)	30.34 (.61)
9	215.97 (.21)	216.77 (.21)	184.82 (.24)	147.83 (.30)	67.20 (.67)	65.89 (.68)

Table 3.2k Shear Envelope Values
21600/A-Actual Linds/5580000 - 1.0g Palmdale

Element	Impact .005	Impact .01	Impact .015	Impact .02	Impact .04	Impact .05
2	9.95 (.046)	11.79 (.039)	13.00 (.035)	10.05 (.046)	4.36 (.11)	1.29 (.36)
3	33.11 (.042)	37.69 (.037)	42.04 (.033)	35.00 (.04)	14.86 (.094)	5.07 (.27)
4	68.70 (.033)	78.42 (.03)	81.67 (.029)	69.09 (.034)	30.56 (.076)	11.23 (.21)
5	98.23 (.033)	122.32 (.026)	128.48 (.025)	108.86 (.029)	48.56 (.066)	21.28 (.15)
6	147.28 (.028)	179.59 (.023)	185.94 (.022)	156.33 (.026)	80.28 (.051)	35.00 (.12)
7	205.12 (.024)	241.81 (.120)	254.14 (.019)	209.85 (.023)	114.22 (.043)	49.91 (.098)
8	414.42 (.016)*	462.76 (.014)*	480.19 (.014)*	401.52 (.016)*	216.72 (.030)*	102.12 (.064)*
9	1305.87 (.017)	1424.01 (.016)	1391.98 (.016)	1179.89 (.019)	433.00 (.052)	310.42 (.072)
10	2894.64 (.019)	2309.52 (.024)	2756.51 (.020)	2241.64 (.024)	886.49 (.061)	793.82 (.069)

Table 3.2% Moment Envelope Values

CASE	1	2	3	4	5	6	7	8	9	10	
Element	Standard Model 21600/A/558000*	216000/6/5580000	216000/A-Weak Links/5580000	216000/A-Actual Links/558000	216000/A/558000	216000/A/55800	54000-216000/A/ 5580000	108000/A/5580000	54000/A/5580000	144/A/580000	Rigid Body Shear
1	1.94 (.20)	2.33 (.16)	1.93 (.20)	1.48 (.26)	1.71 (.22)	1.64 (.23)	1.94 (.20)	1.89 (.20)	2.06 (.19)	168 (.56)*	.55 (.69)
2	5.32 (.22)	6.28 (.18)	5.27 (.22)	4.08 (.28)	4.65 (.25)	4.67 (.25)	5.17 (.22)	5.00 (.23)	5.37 (.21)	1.59 (.72)	1.64 (.70)
3	8.21 (.23)	9.51 (.20)	8.11 (.24)	6.4 (.30)	7.13 (.27)	6.66 (.29)	7.95 (.24)	7.47 (.26)	7.95 (.24)	2.46 (.78)	2.74 (.70)
4	30.51 (.087)*	43.16 (.061)*	10.33 (.26)	22.59 (.12)*	21.5 (.13)*	35.63 (.074)*	29.09 (.091)*	22.75 (.12)*	16.7 (.16)*	4.13 (.64)	3.78 (.70)
5	32.33 (.10)	44.89 (.074)	12.08 (.28)	23.56 (.14)	20.94 (.16)	35.24 (.095)	30.85 (.11)	24.19 (.14)	18.09 (.18)	2.52 (1.33)	4.78 (.70)
6	33.81 (.12)	46.17 (.088)	13.81 (.29)	24.65 (.16)	20.21 (.20)	34.63 (.12)	32.32 (.13)	25.25 (.16)	19.3 (.21)	1.2 (3.37)	5.77 (.70)
7	36.19 (.15)	48.11 (.11)	16.31 (.33)	26.56 (.20)	19.18 (.28)	33.27 (.16)	34.71 (.16)	26.72 (.20)	20.7 (.26)	3.77 (1.46)	7.7 (.70)
8	89.65 (.21)	99.44 (.19)	38.89 (.47)	77.33 (.24)	45.68 (.41)	16.06 (1.15)	88.6 (.21)	80.49 (.23)	72.55 (.25)	1.9 (9.7)	26.35 (.70)
9	154.84 (.29)	196.84 (.23)	76.05 (.6)	130.33 (.34)	104.69 (.43)	59.44 (.75)	154.25 (.29)	144.00 (.31)	136.14 (.33)	14.99 (2.99)	64.0 (.70)

Table 3.3a Average Shear

Case	1	2	3	4	5	6	7	8	9	10
1	2.49 (.13) Standard Model 216000/A/5580000	4.2 (.11) 216000/6/5580000	3.48 (.13) 216000/A-Weak Links/ 5580000	2.66 (.17) 216000/A-Actual Links/5580000	3.08 (.15) 216000/A/558000	2.95 (.16) 216/A/55800	3.5 (.13) 54000-216000/A/ 5580000	3.4 (.13) 108/A/5580000	3.7 (.12) 54000/A/5580000	1.22 (.38) 144/A/5580000
2	13.07 (.11)	15.52 (.09)	12.98 (.11)	9.97 (.14)	11.46 (.12)	10.89 (.13)	12.79 (.11)	12.41 (.11)	13.34 (.10)	3.98 (.35)
3	27.84 (.084)	32.61 (.072)	27.57 (.085)	21.49 (.11)	24.27 (.095)	22.88 (.10)	27.03 (.086)	25.87 (.090)	27.64 (.084)	8.24 (.23)*
4	76.67 (.041)	101.66 (.031)	44.05 (.073)	53.27 (.060)	42.70 (.075)	61.76 (.052)	73.51 (.044)	60.75 (.053)	53.27 (.06)	5.34 (.60)
5	128.33 (.032)	173.5 (.023)	63.42 (.064)	90.61 (.044)	73.87 (.055)	117.71 (.034)	122.88 (.033)	99.44 (.041)	81.62 (.05)	6.44 (.63)
6	182.49 (.027)	247.33 (.02)	85.06 (.057)	130.05 (.038)	105.84 (.046)	172.96 (.028)	174.59 (.028)	139.34 (.035)	112.35 (.044)	5.96 (.82)
7	356.2 (.018)*	477.5 (.014)*	162.12 (.040)*	257.21 (.025)*	197.77 (.033)*	332.15 (.02)*	341.19 (.019)*	268.08 (.024)*	211.70 (.031)*	12.3 (.53)
8	931.51 (.024)	1099.84 (.02)	426.96 (.052)	796.52 (.028)	362.92 (.062)	331.06 (.068)	917.52 (.024)	739.76 (.030)	648.87 (.035)	11.27 (1.99)
9	1985.83 (.027)	2264.2 (.024)	961.01 (.057)	1718.76 (.032)	1010.65 (.054)	150.69 (.36)	1982.21 (.027)	1781.8 (.031)	1583.49 (.034)	109.85 (.50)

Table 3.3b Average Moment

Element	Impact .005	Impact .01	Impact .015	Impact .02	Impact .04	Impact .05
1	4.24 (.09)*	8.56 (.044)*	4.65 (.082)*	4.44 (.086)*	2.03 (.19)	.96 (.40)
2	9.96 (.12)	18.52 (.062)	11.09 (.10)	11.18 (.10)	5.0 (.23)	2.65 (.43)
3	14.95 (.13)	25.25 (.076)	16.67 (.115)	16.6 (.12)	7.92 (.24)	4.17 (.46)
4	28.45 (.093)	37.99 (.069)	30.63 (.086)	30.47 (.087)	24.4 (.11)*	10.84 (.24)*
5	30.1 (.11)	38.68 (.086)	33.98 (.098)	33.36 (.10)	24.97 (.13)	11.79 (.28)
6	31.24 (.13)	41.22 (.098)	37.65 (.11)	36.17 (.11)	25.14 (.16)	12.68 (.32)
7	35.36 (.15)	45.27 (.12)	43.15 (.13)	41.85 (.13)	25.86 (.21)	14.23 (.38)
8	105.82 (.17)	119.75 (.15)	120.62 (.15)	113.62 (.16)	48.98 (.38)	33.29 (.55)
9	179.46 (.25)	196.43 (.23)	182.30 (.25)	164.85 (.27)	85.03 (.53)	70.33 (.64)

Table 3.3c Average Shear

Element	Impact .005	Impact .01	Impact .015	Impact .02	Impact .04	Impact .05
2	7.63 (.060)	15.40 (.03)	8.37 (.055)	7.98 (.058)	3.66 (.13)	1.72 (.27)
3	25.0 (.056)	47.88 (.029)	28.3 (.049)	28.03 (.050)	12.87 (.11)	6.47 (.21)
4	43.71 (.053)	91.75 (.025)	56.83 (.041)	56.98 (.041)	26.73 (.087)	13.91 (.17)
5	84.49 (.038)	130.46 (.025)	99.02 (.032)	100.52 (.032)	54.62 (.059)	28.59 (.11)
6	127.26 (.032)	186.1 (.022)	151.22 (.027)	150.72 (.027)	91.87 (.044)	46.88 (.087)
7	174.76 (.028)	242.67 (.020)	210.45 (.023)	206.55 (.024)	130.63 (.038)	67.0 (.073)
8	339.04 (.019)*	435.29 (.015)*	413.09 (.016)*	401.58 (.016)*	252.73 (.026)*	135.13 (.048)*
9	1054.1 (.021)	1229.75 (.018)	1231.99 (.018)	1184.71 (.019)	425.43 (.053)	361.03 (.062)
10	2342.9 (.023)	1493.22 (.036)	2572.4 (.021)	2387.3 (.023)	1151.12 (.047)	860.63 (.063)

Table 3.3d Average Moment

CHAPTER 4 - EARTHQUAKE INTENSITIES

4.1 Introduction

From the description of damage, chimneys apparently toppled, slid horizontally, and some slid and were partially rotated. The forces required to produce these conditions are necessary to determine the earthquake intensities. This chapter will define the failure criteria used in this study. The failure criteria are defined as the initiation or onset of i) sliding (shear failure) and ii) cracking or uplift due to overturning moment. The failure forces are therefore forces required to initiate damage.

After defining the failure criteria and obtaining the associated forces, the earthquake intensities will be determined. It follows then that the earthquake intensities will be the intensities required to initiate damage, i.e., lower bound intensities.

4.2 Failure Criteria

a) Shear Failure (Coulomb-Mohr Type Failure)

The forces required to initiate shear failure were obtained by assuming:

- 1) the bond stress at the failure location is zero
- 2) the shear resistance is due to friction developing at the horizontal failure plane, between the brick and mortar. The shear capacity, V_f is given by Eq. (4.1).

$$V_f = \mu W \quad (4.1)$$

where μ = coefficient of friction
 W = total weight of chimney above the failure location.

Sliding occurs at the instant the horizontal inertial forces exceed the frictional capacity, as shown in Figure 4.1. It should be noted that $\mu = 0.7$ was used in this study since it is the average value found in a literature survey [4.1].

The shear capacity or the shear failure forces are shown in Table 4.1.

b) Normal Stress Failure

The normal stress failure criteria is defined as the bending moment that produces a state of normal stress at which zero stress exists along one edge of the horizontal failure plane, Eq. (4.2).

$$\sigma = \frac{M}{S} - \frac{W}{A} = 0$$

$$M = \frac{SW}{A} \quad (4.2)$$

where

S = the least section modulus of cross-section at the failure location

W = total weight of chimney above the failure location

A = cross-sectional area at the failure location.

The zero normal stress state, shown in Figure 4.2, is produced by the moment due to the horizontal inertia force becoming larger than the moment due to the self-weight of the chimney above the failure plane.

In determining the moments required to initiate normal stress failure, it was necessary to make the following assumptions:

- 1) the horizontal inertia force does not exceed the shear capacity at the failure plane;
- 2) the mortar tensile capacity is equal to zero.

The normal stress failure moments are shown in Table 4.2.

4.3 Earthquake Intensities

The earthquake intensity required to initiate damage at a particular node is determined by f_f/f , the ratio of the failure force, to the force from the analysis results. The resulting intensity is expressed in acceleration units, ft/sec^2 . The intensities shown in parentheses in Tables 3.2 are expressed in decimal parts of acceleration due to gravity. The asterisks denote the location of the smallest intensity that would initiate failure.

It should be emphasized that the tabulated intensities would only initiate the defined failure and are therefore lower bound intensities to the 1755 Earthquake. Depending upon the duration and peak ground acceleration of an earthquake, the resulting forces may exceed the failure forces (capacity) for an extended period of time, resulting in inelastic behavior, or even total failure. For this reason it would be necessary to perform an inelastic analysis and define more detailed failure criteria, including inelastic behavior, in future research.

4.3a) Chimney Parameters

When comparing the average intensity required to initiate failure of the standard model with the intensities for the different cases where the elastic modulus of the chimney varied, it is observed that the standard model would fail before the others. Shear failure would generally occur at node 4, element 4, at an average intensity of 0.087g. It should be noted that failure would occur just below the roofline, which is not the location of interest, since the force at node 4, element 4 is due to the chimney mass at node 4 plus the house mass at node 15 (refer to Figure 2.7).

For shear failure to occur just above the roofline, an intensity of 0.23g is required, assuming the other nodes do not fail first. But it is observed that elements 4 through 8 would begin to fail before element 3. Therefore it would be expected that inelastic behavior may account for sliding failure at the roofline.

Normal stress failure would also occur in the standard model before the others, at an average intensity of 0.018g at node 8 (Figure 2.7). For normal stress failure to occur just above the roofline, an intensity of 0.084g would be required. But, as in shear failure, failure would begin at nodes 5 through 10 first.

From Table 3.3b it is observed that the intensity required to initiate normal stress failure slightly increases to 0.031g at node 8, as the modulus decreases, from 216000 ksf to 54000 ksf. The intensity suddenly increases to 0.28g at node 4 as the modulus is reduced to 144 ksf.

From these results it is evident that normal stress failure is more critical than shear failure.

4.3b) House Parameters (except impact)

Case 2, where the house mass was increased, would fail in shear at node 4, element 4, at an average intensity of 0.61g. This failure also occurs below the roofline. But the normal stress failure is more critical, requiring an average intensity of 0.14g to initiate failure at node 8.

In Case 3, where the chimney-house connection was made very weak, failure in shear would occur at node 1 element 1 at an average intensity of 0.20g. The normal stress failure would occur at node 8 at an average intensity of 0.04g.

In Case 4, where the actual member sizes were used in the chimney-house connection, shear failure would occur at node 4, element 4, at an average intensity of 0.12g. Normal stress failure would occur at node 8 at an average intensity of 0.025g.

As in the chimney parameter cases, failure would be initiated at several other locations, before the location just above the roofline. And similarly, inelastic behavior may account for failure just above the roofline.

From these results it is observed that an intensity of 0.04g would initiate normal stress failure in any of these cases.

4.3c) Ground Parameters

For the cases of reduced rocking spring stiffness, the average intensity required to initiate failure is larger than that for the standard model. For the case of 10% standard rocking spring stiffness, the average intensity for normal stress failure is 0.033g, while for the 1% standard rocking spring case the intensity required to initiate failure is 0.02g at node 8.

From inspection of Tables 3.2 it is evident that the Palmdale Earthquake would initiate damage before the other earthquakes. As mentioned in Chapter 3, this is primarily due to the higher spectral values in the digitized accelerogram.

4.3d) Impact

From Table 3.3c the case with the gap size of 0.01' is the critical case, requiring the smallest intensity to initiate failure, when compared

to the other impact cases. The average intensity required to initiate normal stress failure is 0.015g at node 8. It should be noted that as the forces are scaled down to an intensity of 0.015g the gap size must also be reduced by the same factor. The corresponding gap size would therefore be 0.00015'. This implies that if there is even the slightest bit of independent movement between the house and chimney, the forces in the chimney can be increased by as much as 2.8 times the case where the actual member sizes were used in the non-impact chimney-house connection. The effect of a gap in the chimney-house connection, therefore, appears to be a very important consideration in determining chimney damage due to earthquakes.

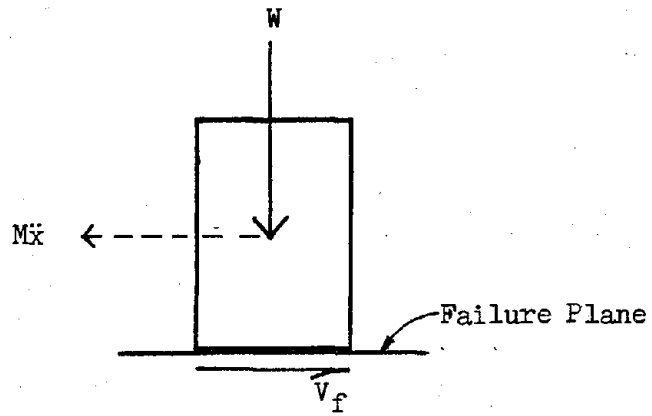


Figure 4.1 Shear Failure

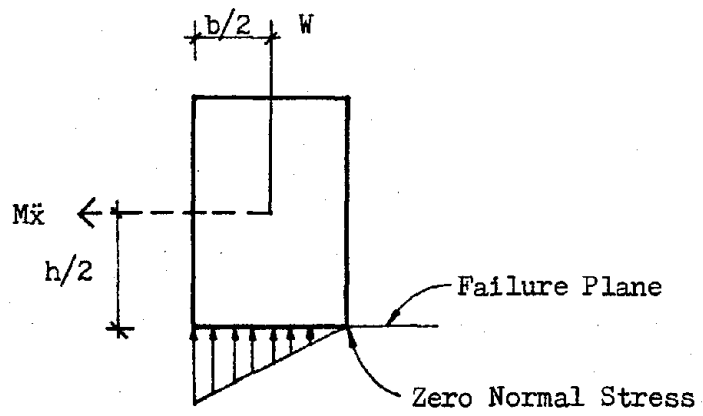


Figure 4.2 Normal Stress Failure

TABLE 4.1		
Element	Node	Failure Force(kips)
1	2	.38
2	3	1.15
3	4	1.92
4	5	2.64
5	6	3.34
6	7	4.04
7	8	5.4
8	9	18.45
9	10	44.82

TABLE 4.2	
Node	Failure Moment(ft-kips)
1	.46
2	1.39
3	2.33
4	3.2
5	4.06
6	4.90
7	6.55
8	22.41
9	54.42

CHAPTER 5 - CONCLUSIONS AND RECOMMENDATIONS

5.1 Conclusions

A pre-1755 heavy-timber frame house with a masonry chimney has been analyzed to determine 1) dynamic response characteristics, ii) force levels in the structure subjected to three earthquake motions, iii) forces required to initiate damage and iv) the approximate lower bound intensity motions of the 1755 Earthquake.

A standard analytical model was developed and a parametric study was performed to understand the effects of the several chimney, house and ground parameters involved in the dynamic analysis

i) From the free vibration analysis it was determined that the fundamental frequencies of the various models were quite high. The fundamental frequency of the standard model was determined to be about 12 Hz. The free vibration analysis of a case where the chimney-house connection was made very weak revealed that the fundamental frequency of the house was approximately 5 Hz and chimney alone was 18.5 Hz.

Once the frequencies and mode shapes were determined, participation factors were computed. The participation factors indicated that the higher modes contribute to the total response of the structure. This rather unusual behavior is due to the concentration of mass in the lower, rigid portion of the chimney.

ii) The dynamic analysis of the standard model revealed that the Palmdale Earthquake was, in general, more severe than El Centro or Ferndale. This is primarily due to the higher spectral values in the short period range of the digitized accelerogram. A comparison of the dynamic analysis and an

assumed rigid body motion case revealed the amount of dynamic amplification in the dynamic response results. It was observed that forces were amplified by at least a factor of 3 when the elastic modulus of the chimney varied. When the chimney and house were allowed to move independently (case 3), the dynamic amplification factor became as large as 3.5 at the top element.

When the foundation rocking spring was reduced, a peculiar variation in force levels of the chimney, inside the house, was observed. The peculiar variation is due to the higher modes of the house, causing some additional lateral load on the chimney.

When there was a gap in the chimney-house connection, it was observed that shear forces increased by as much as 15 times the rigid body shear forces.

iii) The chimney was assumed to fail in one of two possible modes: shear failure and normal stress failure. The shear failure forces are based on the assumption that the coefficient of friction μ between the brick and mortar was 0.7. Shear failure is assumed to occur at the instant frictional resistance, μW , is exceeded, where μ is the coefficient of friction between the brick and mortar and W is the total weight above the failure plane.

Normal stress failure occurs when zero stress exists along one edge of the horizontal failure plane.

iv) The earthquake intensities, f_f/f , the ratio of the failure force to the force from the parametric study results, were computed for the various models. Normal stress failure was always the most critical, requiring a smaller intensity, at a particular node, to initiate failure.

An intensity of .031g is required to initiate normal stress failure in the various chimney parameter models (except for the case where the elastic modulus is reduced to 144 ksf).

An intensity of 0.10g would initiate normal stress failure in the various house parameter models.

For the cases of reduced rocking spring stiffness, an intensity of 0.02g would initiate normal stress failure at node 8.

The impact studies reveal that an intensity of 0.048g would initiate normal stress failure at node 8 for the various gap sizes studied.

The earthquake intensity results indicate that, in general, intensities in the range of 0.015g to 0.04g would initiate normal stress failure in any of the models investigated. It may therefore be concluded that, if the 1755 Earthquake were in the 0.015g to 0.04g intensity range, it would have initiated damage in any one of the various models analyzed.

5.2 Recommendations

In determining earthquake intensities from chimney damage reports, it is of primary interest to understand the damage process. The damage process must then be defined in terms (criteria) of forces so that reasonable estimates of the intensity can be made. The simple failure criteria employed in this study can be improved by allowing the members to yield, since the failure process is an inelastic phenomenon.

To better understand the entire failure process, it is also necessary to investigate both transverse and longitudinal directions of the system. Although an estimate of the transverse stiffness of the house was made, the effects of exterior wall openings, and interior partions, should be studied.

The stiffness in the longitudinal direction may have a significant effect on damage to chimneys, and should therefore be studied.

A study of the impact problem in the chimney-house connection is also an area in which future work should focus. Perhaps modeling the chimney top as a rigid block resting upon a pedestal, subjected to an instantaneous base motion, may be a suitable approach.

And finally, the procedure for determining earthquake intensities should be verified by selecting a modern earthquake where chimney damage has been reported and the intensity is known.

APPENDIX A

METHOD FOR PREDICTING THE LATERAL STIFFNESS AND
STRENGTH OF MULTI-STORY INFILLED FRAMES [2.4]

The characteristic of the infilled frame, λ , for a rectangular frame is given by,

$$\lambda = \sqrt[4]{[(E_c t \sin 2\theta)/(4EIh)]} \quad (1)$$

and h , represents the relative stiffness of the infill to the column. The relation between α/h , the length of contact, and h , is shown in Eq. 2.

$$\frac{\alpha}{h} = \frac{\pi}{2h} \quad (2)$$

The length of contact can therefore be determined using Eq. 2 after λ , has been determined by Eq. 1. Substituting values,

$$\frac{\alpha}{h} = 0.47$$

The effective width of the equivalent strut, w/d , is then determined from experimental curves shown in figure 1. The effective width is a function of the infill stiffness and dimensions. From the curves, $w/d = 0.10$, where d is the

diagonal length of the infill panel. Therefore,

$$\begin{aligned} w &= 0.1d \\ &= (0.1)(23.2) \\ w &= 2.3' \end{aligned} \quad (3)$$

The equivalent timber strut cross-sectional area is given by,

$$\begin{aligned} A &= \frac{E_c w t}{E} \\ &= \frac{(1.5)(10^6)(2.3)(12)(4)}{(10^6)(144)} \end{aligned}$$

$$A = 1.15 \text{ sq. ft.}$$

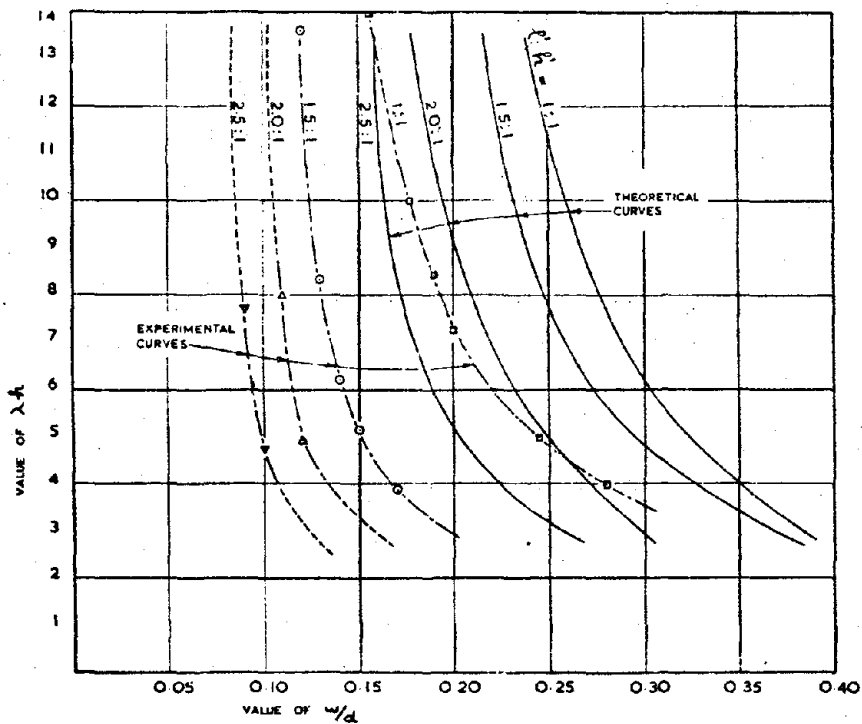


Figure A.1 Effective Width as a Function of λh

NOTATION

d = Diagonal length of infill = 23.2'

E_c = Elastic modulus of infill = $1.5(10^6)$ psi

E = Elastic modulus of frame = 10^6 psi

h = Height of column between center-lines of beams = 8.0'

h' = Height of infill = 7.5'

I = Second moment of area of column = 1296 in⁴

l' = Length of infill = 22'

l = Length of beams between center-lines of columns = 22.87'

t = Thickness of infill = 4 in.

w = Effective width of infill

α = Length of contact

θ = Slope of the infill diagonal to the horizontal = 18.8

λ = Characteristic of the infilled frame; for a rectangular frame

$$\lambda = \sqrt[4]{[(E_c t \sin 2\theta)/(4EIh)]}$$

APPENDIX B

SPRING CONSTANTS FOR RIGID RECTANGULAR
BASE RESTING ON ELASTIC HALF-SPACE [2.6]

For rocking motion:

$$k_{\phi} = \frac{G}{1 - \mu} \beta_{\phi} B L^2 \quad (1)$$

where,

$$\begin{aligned} \mu &= 0.4 \text{ for moderately saturated soils} \\ L &= 14.33' \\ B &= 9.33' \\ \beta_{\phi} &= 0.56, \text{ from Figure B.1} \end{aligned}$$

Therefore,

$$\begin{aligned} k_{\phi} &= \frac{G}{1 - 0.4} (0.56)(9.33)(14.33^2) \\ &= 1788G \text{ (ft. units)} \end{aligned}$$

The shear wave velocity is used to determine the shear modulus, G.

$$G = \rho C_s^2 \quad (2)$$

where,

$$\begin{aligned} C_s^2 &= \text{Shear wave velocity} = 1200 \text{ ft/sec} \\ &\quad \text{(for good stiff till)} \\ \rho &= \text{mass density} = \gamma/g \\ \gamma &= \text{unit weight of soil} = 135 \text{ lbs/ft}^3 \\ g &= \text{acceleration of gravity} = 32.2 \text{ ft/sec}^2 \end{aligned}$$

Therefore,

$$\begin{aligned} G &= (4.19)(1200^2) \\ &= 6.04(10^6) \text{ lbs/sq. ft.} \end{aligned}$$

The rocking spring constant calculated above is for a solid rigid rectangular base, but the actual base is not solid.

Assume that the spring constant is directly proportional to the ratio, $I_{\text{actual}} / I_{\text{solid}}$.

$$\begin{aligned}
 I_{\text{solid}} &= \frac{bh^3}{12} \\
 &= \frac{(9.33)(14.33^3)}{12} \\
 &= 2288 \text{ ft}^4
 \end{aligned}$$

$$I_{\text{actual}} = 1183 \text{ ft}^4$$

Therefore,

$$\begin{aligned}
 k_{\phi} &= \frac{(1788)(6.04)(10^6)(1183)}{2288} \\
 &= \underline{5.58(10^6) \text{ kip-ft/rad}}
 \end{aligned}$$

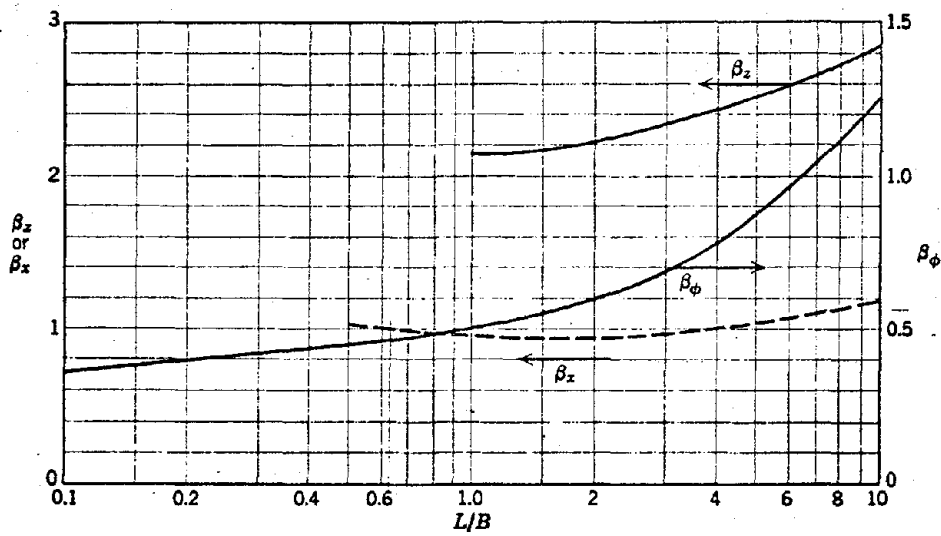


Figure B.1 Spring constant coefficients for rectangular foundations

NOTATION

B = Width of foundation along axis of rotation = 9.33'

C_s = Shear velocity = 1200 ft/sec (for good stiff till)

G = Shear modulus

g = Acceleration of gravity = 32.2 ft/sec²

γ = Unit weight of soil = 135 lbs/ft³

I = Second moment of area

k_ϕ = Rocking spring constant

L = Length of foundation in plane of rotation = 14.33'

ρ = Mass density

μ = Poisson's ratio

APPENDIX C

GAP MODEL TIME STEP ACCURACY AND
SCALING OF RESULTS

Tables C.1, C.2 and C.3 compare results of the gap model when integrated at different time steps. Table C.1 compares time steps of 0.001 sec. and 0.005 sec. Table C.2 compares time steps of 0.0008 sec. and 0.001 sec. Table C.3 compares time steps of 0.0008 sec. and 0.0005 sec. Note that the results are approximately the same.

Table C.4 indicates that results of the gap model can be scaled. For a gap size of 0.01', subjected to a peak ground acceleration of 1.0g, the results are 10 times larger than a model with a gap size of 0.001' subjected to a 0.01g peak ground acceleration.

TABLE C.1		
Element	SHEAR FORCES Gap Size = 0.00001' El Centro 1.0g	
	0.001 sec.	0.005 sec.
1	1.24	1.24
2	3.20	3.52
3	4.90	5.61
4	25.87	24.89
5	27.20	26.46
6	28.54	27.92
7	30.91	30.53
8	92.63	95.19
9	152.76	156.91

TABLE C.2		
Element	SHEAR FORCES Gap size = 0.001' El Centro 1.0g	
	0.0008 sec.	0.001 sec.
1	15.4	14.05
2	29.9	28.24
3	39.1	39.42
4	50.3	49.48
5	48.2	49.17
6	51.8	46.68
7	52.5	54.19
8	122.3	129.97
9	212.0	208.91

TABLE C.3		
Element	SHEAR FORCES Gap Size = 0.01' Palmdale 1.0g	
	0.0008 sec.	0.0005 sec.
1	6.55	6.07
2	15.83	15.55
3	22.64	23.11
4	38.56	38.49
5	40.60	41.25
6	42.70	43.08
7	48.84	48.91
8	141.58	139.41
9	216.77	216.80

Element	TABLE C.4	
	SHEAR FORCES	
	Gap = 0.01' El Centro 1.0g	Gap = 0.001' El Centro 1.0g
1	15.38	1.54
2	29.91	2.99
3	38.83	3.91
4	50.29	5.03
5	48.21	4.82
6	51.81	5.18
7	52.59	5.25
8	122.43	12.23
9	212.16	21.20

REFERENCES

Chapter 1

1. Okamoto, S., Introduction to Earthquake Engineering, John Wiley & Sons, 1973, p. 31.
2. Weston Geophysical Research, Inc., Historical Seismicity of New England, March 1977, Docket No. 50-471.

Chapter 2

1. Busch, C., Residential Construction in Boston at the Time of the Cape Ann Earthquake of 1755, Internal Report, M.I.T., Dept. of Civil Engineering, June 1979.
2. Jenison, P., "The Availability of Lime and Masonry Construction in New England: 1630-1733," The Bulletin of the Society for the Preservation of New England Antiquity, Vol. LXVII, Nos. 1-2, Sum.-Fall, 1976, Serial No. 245-246.
3. Dahan, E., Preliminary Analysis: 1755 Earthquake, Internal Report, M.I.T., Dept. of Civil Engineering, Sept. 1978.
4. Smith, B., "Methods for Predicting the Lateral Stiffness and Strength of Multi-story Infill Frames," Build. Sci., Vol. 2, pp. 247-257, 1967.
5. Scholl, R.E., and Farhoomand, I., Dynamic Response Characteristics of One-Story Test Structures, John A. Blume and Associates, JAB 99-49, July 1972.
6. Lambe, T.W., and Whitman, R.V., Soil Mechanics, John Wiley & Sons, 1969, pp. 231-232.
7. Kanaan, A.E., and Powell, G.H., User's Guide for DRAIN 2-D, A General Purpose Computer Program for Dynamic Analysis of Inelastic Plane Structures, Earthquake Engineering Research Center, Univ. of California, Berkeley, Sept. 1973.
8. Moler, C.B., and Stewart, G.W., "An Algorithm for Generalized Matrix Eigenvalue Problems," SIAM J. Numer. Anal., 10, pp. 241-256 (1973).

Chapter 4

1. Mayes, R.L. and Clough, R.W., State of the Art in Seismic Shear Strength of Masonry—An Evaluation and Review, Earthquake Engineering Research Center, College of Engineering, Univ. of California, Berkeley, CA, Report No. EERC 75-21, October 1975.

